THE ASTROPHYSICAL JOURNAL, 467:551–578, 1996 August 20

LARGE-SCALE OUTFLOWS IN EDGE-ON SEYFERT GALAXIES. II. KILOPARSEC-SCALE RADIO CONTINUUM EMISSION

EDWARD J. M. COLBERT,[1,2] STEFI A. BAUM,[1] JACK F. GALLIMORE,[1,2]
CHRISTOPHER P. O'DEA,[1] AND JENNIFER A. CHRISTENSEN[1]
Received 1996 January 5; accepted 1996 March 8

ABSTRACT

We present deep images of the kiloparsec-scale radio continuum emission in 14 edge-on galaxies (10 Seyfert and four starburst galaxies). Observations were taken with the VLA at 4.9 GHz (6 cm). The Seyfert galaxies were selected from a distance-limited sample of 22 objects (defined in the first paper in this series). The starburst galaxies were selected to be well matched to the Seyferts in radio power, recessional velocity, and galaxy disk inclination angle. All four starburst galaxies have a very bright disk component, and one (NGC 3044) has a radio halo that extends several kiloparsecs out of the galaxy plane. Six of the 10 Seyferts observed have large-scale (radial extent $\gtrsim 1$ kpc) radio structures extending outward from the nuclear region, indicating that large-scale outflows are quite common in Seyferts. Large-scale radio sources in Seyferts are similar in radio power and radial extent to radio halos in edge-on starburst galaxies, but their morphologies do not resemble spherical halos observed in starburst galaxies. The sources have diffuse morphologies, but, in general, they are oriented at skewed angles with respect to the galaxy minor axes. This result is most easily understood if the outflows are AGN-driven jets that are somehow diverted away from the galaxy disk on scales $\gtrsim 1$ kpc. Starburst-driven winds, however, cannot be ruled out. More observational work is needed to determine whether massive star formation is present at high enough rates to drive galactic winds out to kiloparsec scales in Seyfert galaxies.

Subject headings: galaxies: kinematics and dynamics — galaxies: Seyfert — galaxies: starburst — radio continuum: galaxies

1. INTRODUCTION

Optical light from quasars is primarily emitted by the active galactic nucleus (AGN) and not by the host galaxy. Similarly, radio emission from classical radio galaxies is predominantly emission produced by the AGN. However, in Seyfert galaxies, although the AGN is often very luminous when compared with the host galaxy, it may not always dominate the luminosity in a given waveband. For example, in the archetypical Seyfert galaxy NGC 1068, a circumnuclear starburst is quite luminous at infrared (IR; Balick & Heckman 1985) and X-ray (Wilson et al. 1992) wavelengths. Rodríguez-Espinosa, Rudy, & Jones (1987) concluded that most of the far-IR emission from Seyfert galaxies is due to starburst episodes occurring in the galactic envelopes surrounding the active nucleus. This result, coupled with the known correlation between far-IR and radio luminosity for starbursting systems (see, e.g., Helou, Soifer, & Rowan-Robinson 1985), suggests that much of the radio emission in Seyferts might also be produced by circumnuclear starbursts.

Early radio surveys (de Bruyn & Wilson 1976; Meurs & Wilson 1981; Wilson & Meurs 1982) of Seyferts with the Westerbork Synthesis Radio Telescope demonstrated that, in most Seyferts, most of the radio flux is confined to the central region of the galaxy. Large radio structures analogous to jets in radio galaxies were not generally detected, and most of the detected objects were unresolved at this resolution ($\sim 20''$). Soon after the Very Large Array (VLA[3]) became available, Condon et al. (1982) imaged a sample of bright spiral galaxies (some of which were Seyferts) with strong radio sources and argued that the radio emission from the central sources could be explained by synchrotron radiation from supernova remnants (SNRs). However, Wilson & Willis (1980) claimed that the AGN was producing much of the nuclear radio emission.

Subkiloparsec-scale VLA surveys of Seyferts (see, e.g., Ulvestad & Wilson 1989 and references therein) later showed that nuclear sources in Seyferts come in several types of morphological classes. "Linear" (L-type) radio structures $\lesssim 1$ kpc are found in $\sim 20\%$–30% of Seyfert galaxies (Ulvestad & Wilson 1989; Kukula 1993). "Diffuse" (D-type) central radio structures were also found, at about the same frequency of occurrence. Some Seyferts have both L and D components. Compact (unresolved, $\lesssim 1''$) nuclear radio sources were present in many of the objects. Wilson (1988) suggested that the diffuse radio components were produced by star formation activity, while the compact and linear radio components were produced by the AGN.

The radio powers of Seyfert galaxies are $\sim 10^{22}$–10^{25} W Hz^{-1} at centimeter wavelengths (see, e.g., Meurs & Wilson 1984). Normal spirals (i.e., spirals that do not have AGNs) have radio powers that are, on average, several orders of magnitude lower ($\sim 10^{20}$–10^{23} W Hz^{-1}; e.g., Hummel 1981). Hummel (1981) found that, in normal spirals, most ($\gtrsim 90\%$) of the total radio power comes from the disk component. However, central radio sources were also found in

[1] Space Telescope Science Institute, 3700 San Martin Drive, Baltimore, MD 21218.
[2] Department of Astronomy, University of Maryland, College Park, MD 20742.

[3] The VLA is part of the National Radio Astronomy Observatory (NRAO), which is operated by Associated Universities, Inc., under contract with the National Science Foundation.

some normal spirals. Seyfert nuclei are usually found in spiral hosts, so one would expect the total radio emission from Seyfert galaxies to consist of at least (1) a central "nuclear" component produced by the AGN, (2) another central component, probably produced by SNRs in the nuclear region of the host galaxy (cf. Condon 1992), and (3) a "disk" component from the host galaxy.

A fourth component of radio emission in Seyferts has also been identified in several objects. Hummel, van Gorkom, & Kotanyi (1983) showed that, in large-scale[4] maps of five edge-on galaxies (two were later identified as Seyferts and the other three as LINERs), "anomalous" components extend out of the disk and appear to be coming from the nuclear region. In a more recent study of 13 Seyferts selected for large-scale radio or optical emission, Baum et al. (1993) found large-scale, extranuclear components in 12 objects and showed that the radio sources were preferentially aligned with the minor axes of the galactic disks. They suggested that the sources could be produced by galactic winds powered by circumnuclear starbursts and also discussed the possibility that they are produced by AGN-driven outflows. Although several cases of such extraplanar emission have been noted in the literature, a systematic study of these features in Seyfert galaxies has never been published. One would like to conduct such a study in order to determine whether these large-scale radio structures are common in Seyfert galaxies, understand their radio properties, and investigate whether they might be produced by the AGN or circumnuclear star formation activity.

This is Paper II from a study of large-scale outflows (LSOs) in a complete, distance-limited sample (see Colbert et al. 1996, hereafter Paper I) of edge-on Seyfert galaxies. In Paper I, we used Hα + [N II] images and/or minor axis optical spectra of 22 edge-on Seyfert galaxies to show that LSOs are likely to be present in at least one-fourth of all Seyferts. In this paper, we present large-scale VLA maps of 10 of the 22 galaxies in our complete sample. Our maps allow us to search for emission at low surface brightness levels ($\gtrsim$0.05 K at 6 cm), which is several times better than those of most published large-scale radio maps of Seyferts. We also present large-scale radio maps for a comparison sample of four edge-on starburst galaxies, selected to be well matched to the sample Seyferts.

Observations and data reduction techniques are described in § 2. In § 3, we present results for individual objects and list properties of the observed radio sources. In § 4, we describe the large-scale radio structures from Seyferts in our complete sample and compare their properties with those of radio jets and lobes in classical radio galaxies and radio halos in starburst galaxies. We then discuss AGN and starburst origins for the large-scale radio structures. A Hubble constant of 75 km s^{-1} Mpc^{-1} is assumed throughout this paper.

2. OBSERVATIONS AND DATA REDUCTION

A total of 16 galaxies were observed (12 Seyferts and four starbursts). The Seyfert galaxy Mrk 577 was not detected. We observed the Seyfert galaxy IRAS 13197−1627 but later discovered it was not associated with the edge-on spiral galaxy MCG −3-34-63 (see Appendix for details and radio maps of this object). Thus, in this paper we present radio maps for 10 edge-on Seyfert galaxies and four edge-on starburst galaxies.

Observations were made at 6 cm (central frequency 4860.1 MHz) with the VLA on 1994 June 12, while the array was in C-configuration. The effective bandpass was 100 MHz, and integration times were $\sim$45 minutes per galaxy.

Calibration and reduction of the data was performed using the NRAO AIPS data reduction package. Visibility data were flux density calibrated from observations of 3C 286 and phase calibrated using frequent observations of nearby VLA point-source calibrators.

For all objects detected, the visibility data were improved using several cycles of self-calibration and mapping (see Perley, Schwab, & Bridle 1989). The shortest spacings are $\sim$1 kλ, so the images are sensitive to structure $\lesssim$3′ in size.

Several types of CLEANed maps were made from the final self-calibrated visibilities. All maps presented in this paper have been restored with circular Gaussian beams. Circular beams were chosen over elliptical beams so that we could measure geometrical properties of the extended emission directly from the maps. Maps with beam size 5″ FWHM (full width half-maximum), the approximate size of the synthesized beam, have sensitivities $\sim$20–25 μJy beam^{-1}, which corresponds to a brightness temperature of $\sim$50 mK. These maps are hereafter referred to as the "normal" maps. Next, a set of "hi-res" maps was made by restoring the image with a circular Gaussian beam with FWHM = 3″. These maps were used for determining the structure of the nuclear emission and for estimating the nuclear radio flux. Finally, we used a 20 kλ Gaussian taper on the visibility data to produce "tapered" maps (circular beam, FWHM = 10″), which are more sensitive to large-scale structure. The normal and tapered maps were made using natural weighting, and the hi-res maps were made using uniform weighting.

Archival data from observations described in Edelson (1987) were retrieved from the VLA archives, recalibrated, and reduced to maps using self-calibration and CLEANing techniques. These data were taken at both 1.46 and 4.89 GHz (20 and 6 cm), when the array was in D-configuration. Although the beam sizes in these maps are considerably larger ($\sim$20″ and 60″ FWHM, respectively), the maps are sensitive (rms noise at 6 cm $\sim$ 0.1 mJy beam^{-1} $\sim$ 20 mK) to structure $\gtrsim$3′ and so were used to supplement the 6 cm C-configuration maps. All of the maps of the Seyferts in our complete sample (Paper I) are unresolved in these data, except for those of NGC 4235. A low-resolution 1.46 GHz map of NGC 4235 from this D-configuration data is presented in § 3.

3. RESULTS

A list of the 22 edge-on Seyferts in our complete distance-limited sample is given in Table 1. The 10 Seyferts for which we have obtained new radio maps are noted in the second column. Host galaxy types, optical positions, axial ratios, and recessional velocities for these galaxies can be found in Table 1 of Paper I. Here we list assumed distances to the galaxy, total 6 cm radio power P_6, total far-infrared (FIR) luminosity L_{FIR}, and μ, the logarithm of the ratio of 60 μm flux to total 6 cm radio flux.

The mean value of log P_6 for our complete sample of Seyferts is 21.4 log W Hz^{-1}, which is comparable to total

[4] In this paper, the term "large-scale" refers to scales $\gtrsim$1 kpc, unless otherwise noted.

TABLE 1

COMPLETE STATISTICAL SAMPLE OF EDGE-ON SEYFERT GALAXIES

Galaxy Name	New Map?	Seyfert Type	D[a] (Mpc)	P_6[b] (log W Hz^{-1})	References[c]	L_{FIR}[d] (log ergs s^{-1})	μ[e]
IC 1657	No	2	47.4	21.35	1	43.69	2.52
UM 319	Yes	2	63.1	21.43	2	43.60	2.47
Mrk 993	Yes	2	62.1	21.03	2	43.08	2.10
Mrk 577	No	2	69.1	<19.84	2	...	...
Ark 79	Yes	2	68.8	21.55	2	...	...
NGC 931	No	1	66.6	21.52	3	43.94	2.66
NGC 1320	Yes	2	36.0	20.74	2	43.22	2.80
NGC 1386	No	2	20.0	21.01	3	43.18	2.45
NGC 2992	Yes	2	30.9	22.00	2	43.81	2.09
MCG −2-27-9	Yes	2	62.0	20.65	2	43.21	2.69
NGC 4235	Yes	1	32.1	21.03	2	42.36	1.56
NGC 4388	No	2	33.6	21.78	3	43.88	2.37
NGC 4602	Yes	1.9	34.0	20.92	2	43.65	2.90
NGC 4945	No	2	6.7	22.35	4	44.02	1.94
IC 4329A	No	1	63.9	22.22	3	43.68	1.81
NGC 5506	Yes	2	24.2	22.10	2	43.44	1.67
ESO 103-G35	No	2	53.1	...	...	43.48	...
NGC 6810	No	2	26.1	...	...	43.93	...
IC 1368	Yes	2	52.2	21.53	2	43.82	2.59
IC 1417	No	2	57.5	...	...	43.14	...
NGC 7410	No	2	23.3	20.29	5	42.60	2.38
NGC 7590	No	2	21.3	21.42	6	43.45	2.21

NOTE.—Optical positions, axial ratios, and recessional velocities for these objects are listed in Paper I, Table 1.

[a] Assumed distance in Mpc. Except for NGC 1386 and NGC 4945, distances were calculated from recessional velocities listed in RC3 (see Paper I), using $H_0 = 75$. The distance to NGC 1386 was taken as 20.0 Mpc (the distance to the Fornax cluster), and a distance of 6.7 Mpc was assumed for NGC 4945.

[b] Total radio power at 6 cm (4.89 GHz). Fluxes measured at other frequencies were converted to fluxes at 4.89 GHz assuming $S_\nu \propto \nu^{-0.75}$.

[c] REFERENCES.—(1) 1.42 GHz VLA B/C configuration, Unger et al. 1981; (2) this paper; (3) 4.89 GHz VLA D configuration, Rush et al. 1995; (4) 4.75 GHz Parkes, Harnett et al. 1989; (5) 1.49 GHz VLA D configuration, Condon 1987; (6) 2.70 GHz single-dish, Wright 1974.

[d] Far-infrared luminosities, determined from *IRAS* fluxes using the method described in Fullmer & Lonsdale 1989. Fluxes were taken from Rush, Malkan, & Spinoglio 1993 when available; otherwise, fluxes are from Moshir et al. 1992 (as listed in the NASA Extragalactic Database [NED]).

[e] Logarithm of ratio of 60 μm flux density to total 6 cm flux density.

radio powers for larger samples of Seyferts (see, e.g., Edelson 1987; Kukula et al. 1995). The Seyferts observed by Baum et al. (1993) are, on average, higher in total radio power by a factor of ~ 3 (mean value of log P_6 = 21.8 log W Hz^{-1}), which can be explained by their selection criterion to observe Seyferts that previously had evidence for large-scale radio emission. Since our sample of Seyferts was selected by distance, our results are more representative for all Seyferts, not just radio-loud ones.

In Table 2, for each of the four edge-on starburst galaxies, we list galaxy morphologies, axial ratios, recessional velocities, assumed distances, P_6, L_{FIR}, and μ. These galaxies were selected to be well matched to the Seyferts in radio luminosity, axial ratio, and recessional velocity.

Literature searches were done for all 26 galaxies (22 Seyferts and four starbursts). We did not find any information about possible radio emission from the Seyfert galaxies ESO 103-G35, NGC 6810, and IC 1417. Radio observations of the other galaxies are discussed in the following two subsections. In § 3.1, we present our new radio maps of 10 of the 22 Seyfert galaxies and discuss results from previous radio observations. In § 3.2, we present new radio

TABLE 2

COMPARISON SAMPLE OF EDGE-ON STARBURST GALAXIES

Galaxy Name	Galaxy Type[a]	log R_{25}[b]	cz[b] (km s^{-1})	D[b] (Mpc)	P_6[c] (log W Hz^{-1})	L_{FIR}[d] (log ergs s^{-1})	μ[e]
UGC 903	S?	0.70	2518	33.6	21.42	43.75	2.57
NGC 1134	S?	0.46	3644	48.6	21.90	44.13	2.48
NGC 3044	SB(s)c? sp	0.84	1292	17.2	21.12	43.30	2.42
NGC 7541	SB(rs)bc: pec	0.45	2681	35.7	21.95	44.24	2.52

[a] Morphological type, taken from the NASA Extragalactic Database (NED).

[b] Axial ratios (R_{25}) were taken from RC3. Recessional velocities (cz) are optical (or 21 cm, when available) velocities listed in RC3, unless otherwise noted. Distances were calculated from recessional velocities, using $H_0 = 75$.

[c] Total radio power at 6 cm (4.89 GHz), measured from the radio maps presented in this paper.

[d] Far-infrared luminosities, determined from *IRAS* fluxes using the method described in Fullmer & Lonsdale 1989. Fluxes were taken from Moshir et al. 1992 (as listed in the NASA Extragalactic Database [NED]).

[e] Logarithm of ratio of 60 μm flux density to total 6 cm flux density.

maps (and discuss previous radio observations) of the four starburst galaxies.

3.1. *Individual Objects: Seyfert Galaxies*

3.1.1. *IC 1657*

We did not obtain radio images of IC 1657. Unger et al. (1989) observed this galaxy with the VLA in a hybrid B-C configuration but do not show a map of the radio emission. They quote a total flux of 21 mJy at 1.4 GHz.

3.1.2. *UM 319*

In Figure 1*a*, we show contour maps of the radio emission from UM 319 overlaid on an optical image. The large-scale structure extends out to $\sim 10''$ (3 kpc) to the southeast and out to $\sim 5''$ to the northwest, which is not quite out of the disk, in projection. From the hi-res map, one can notice that the radio morphology roughly appears linear in structure, extending along P.A. $\approx 125°$. Such a "linear" radio morphology is suggestive of a bisymmetric nuclear outflow, but follow-up observations at higher resolution are necessary to determine the radio morphology on smaller scales. Additional observations at lower surface brightnesses (or lower frequencies, if the extranuclear component has a steep spectrum) would be useful for determining if the observed extranuclear emission extends out further from the nucleus.

3.1.3. *Mrk 993*

A contour map of the radio emission from Mrk 993 is shown over an optical image of the galaxy in Figure 1*b*. The central radio source is unresolved in our maps. It is also unresolved in 8.4 GHz maps (VLA, A- and C-configuration) presented in Kukula et al. (1995).

3.1.4. *Mrk 577*

We observed Mrk 577 but did not detect it (3 σ upper limit 0.12 mJy at 4.9 GHz). Previous workers (see, e.g., Kojoian et al. 1980; Mulchaey 1995) have observed this galaxy but also have failed to detect it.

3.1.5. *Ark 79 (UGC 1757)*

Contour maps of the radio emission from Ark 79 are shown in Figure 1*c*. The nuclear radio source is slightly resolved (see hi-res map) and extends southward and slightly westward along the disk. The extranuclear emission does not quite extend out of the plane of the disk (in projection) but does extend in the general direction of the minor axis. No small-scale maps of the nuclear radio emission from Ark 79 have been published.

3.1.6. *NGC 931 (Mrk 1040)*

We did not obtain radio images of NGC 931. Rush, Malkan, & Edelson (1995) find a flux of 6.2 mJy at 4.9 GHz (VLA, D-configuration) but do not show a map.

3.1.7. *NGC 1320 (Mrk 607)*

Contour maps of the radio emission from NGC 1320 are shown in Figure 1*d*. In addition to the nuclear radio source, we find emission extending out to $\sim 5''$ (0.9 kpc) to the south from the nucleus in P.A. $\approx 180°$ (see hi-res map). The emission also extends slightly northward in the same P.A., and also to the northwest, along the disk. As in UM 319, the emission appears linear but does not extend out of the disk (in projection). Follow-up radio observations would be useful for determining if structure is present on smaller and larger scales.

3.1.8. *NGC 1386*

We did not observe NGC 1386. No extranuclear radio emission is resolved in the large-scale 1.4 GHz radio map presented in Condon (1987). Rush et al. (1995) quote a flux of 21.5 mJy at 4.9 GHz from VLA D-array observations. On small scales, the nuclear radio source is only slightly extended (out to ~ 400 pc) along the galaxy major axis (southwest along P.A. 55°; Weaver, Wilson, & Baldwin 1991; Ulvestad & Wilson 1984). Weaver et al. (1991) present evidence for a nuclear outflow directed along the *major* axis.

3.1.9. *NGC 2992*

In Figure 1*e*, we show contour maps of the radio emission from NGC 2992. The nuclear radio source is surrounded by fainter emission with complex structure extending in nearly all P.A.'s on a scale of $\sim 20''$–$30''$ (3–4.5 kpc). Extraplanar emission to the east and west is noticeable in the normal and tapered images. The large-scale 20 cm map from Hummel et al. (1983, reproduced in Figure 1*e*; see also map in Ward et al. 1980) clearly shows extraplanar emission extending to the east, but this emission is not well imaged in our 4.9 GHz (6 cm) maps. By comparing the map of Hummel et al. with a map made from our data which has the same beam size, we find that the eastern "arm" of radio emission has a very steep spectrum ($\alpha \gtrsim 2$; $S_\nu \propto \nu^{-\alpha}$). On smaller scales, the nuclear morphology consists of a compact source plus surrounding diffuse emission (Ulvestad & Wilson 1984) which resembles a "striking pair of loops" extending $\sim 2''$ (0.3 kpc) north (and south) from the compact nuclear source in P.A. $\sim 0°$ (Wehrle & Morris 1988).

FIG. 1.—Large-scale radio maps of edge-on Seyfert galaxies: Contour maps of the radio emission overlaid on gray-scale plots of the optical emission. The optical images are digitized versions of optical survey plates from the STScI digitized sky survey. See § 2 for a description of the "normal" (beam size $5'' \times 5''$ FWHM), "hi-res" ($3'' \times 3''$ FWHM) and "tapered" ($10'' \times 10''$ FWHM) 6 cm maps. Unless otherwise stated, contour levels are 25 μJy $\times$ -3, 3, 5, 7, and 10, and then successive levels are a factor of 2 larger. (*a*) UM 319. Normal (*left*) and hi-res (*right*) maps. Peak flux densities are 4.4 and 4.0 mJy beam^{-1}, respectively. (*b*) Mrk 993. Normal map. The peak flux density is 2.9 mJy beam^{-1}. (*c*) Ark 79. Normal (*top*) and hi-res (*bottom*) maps. Peak flux densities are 5.2 and 4.4 mJy beam^{-1}, respectively. (*d*) NGC 1320. Normal (*left*) and hi-res (*right*) maps. Peak flux densities are 2.4 and 2.0 mJy beam^{-1}, respectively. (*e*) NGC 2992. Normal map. On facing page, tapered (*left*) map plus reproduction of contours from the 20 cm map (6″ beam) from Hummel et al. (1983) (*right*). Peak flux densities in the normal and tapered maps are 49.3 and 68.4 mJy beam^{-1}, respectively. Contour levels in the 20 cm map are $-$ 2, 2, 4, 7, 10, 20, 30, 50, 70, 90, and 110 mJy beam^{-1} (*f*) MCG $-$2-27-9. Normal map. The peak flux density is 4.5 mJy beam^{-1}. (*g*) NGC 4235. Normal map. On facing page, tapered (*upper*) map plus 20 cm map (beam $58.7'' \times 51.1''$ FWHM, P.A. + 72°) from Edelson (1987) data (*lower*). Peak flux densities in the normal and tapered maps are 5.3 and 5.6 mJy beam^{-1}, respectively. Contour levels in the 20 cm map are 0.4 mJy beam^{-1} $\times$ (3, 5, 7, 10, and 20). (*h*) NGC 4388. Reproduction of the contours from the 6 cm map (beam $5''.6 \times 5''.1$, P.A. $-$ 20°) from Hummel et al. (1983). Contour levels are 0.25, 0.5, 1, 2, 4, 8, 12, and 16 mJy beam^{-1}. (*i*) NGC 4602. Normal map. The peak flux density is 2.0 mJy beam^{-1}. (*j*) NGC 4945. Reproduction of the contours from the 4.75 GHz (6 cm; 4′.6 beam) map from Harnett et al. (1989). Contour levels are 0, 10, 25, 40, 70, 100, 250, 500, 750, 1000, 1250, 1500, 1750, and 2000 mJy beam^{-1}. (*k*) IC 4329A. Reproduction of contours from the 6 cm radio map (beam size $1''.3 \times 1''.2$, P.A. $-$ 31°) of the radio emission from Unger et al. (1987). Contour levels are 19 mJy beam^{-1} $\times$ percentages (2, 4, 6, 8, 16, 30, 40, and 50). (*l*) NGC 5506. Normal (*top*) and tapered (*bottom*) maps. Peak flux densities are 159.9 and 170.4 mJy beam^{-1}, respectively. (*m*) IC 1368. Normal map. The peak flux density is 9.8 mJy beam^{-1}. (*n*) NGC 7410. 20 cm map (48″ beam) from Condon (1987). Contour levels are 0.1 mJy beam^{-1} $\times$ ($-$3, 3, 5, 7, 10, 20, and 40. The peak flux density is 5.4 mJy beam^{-1}.

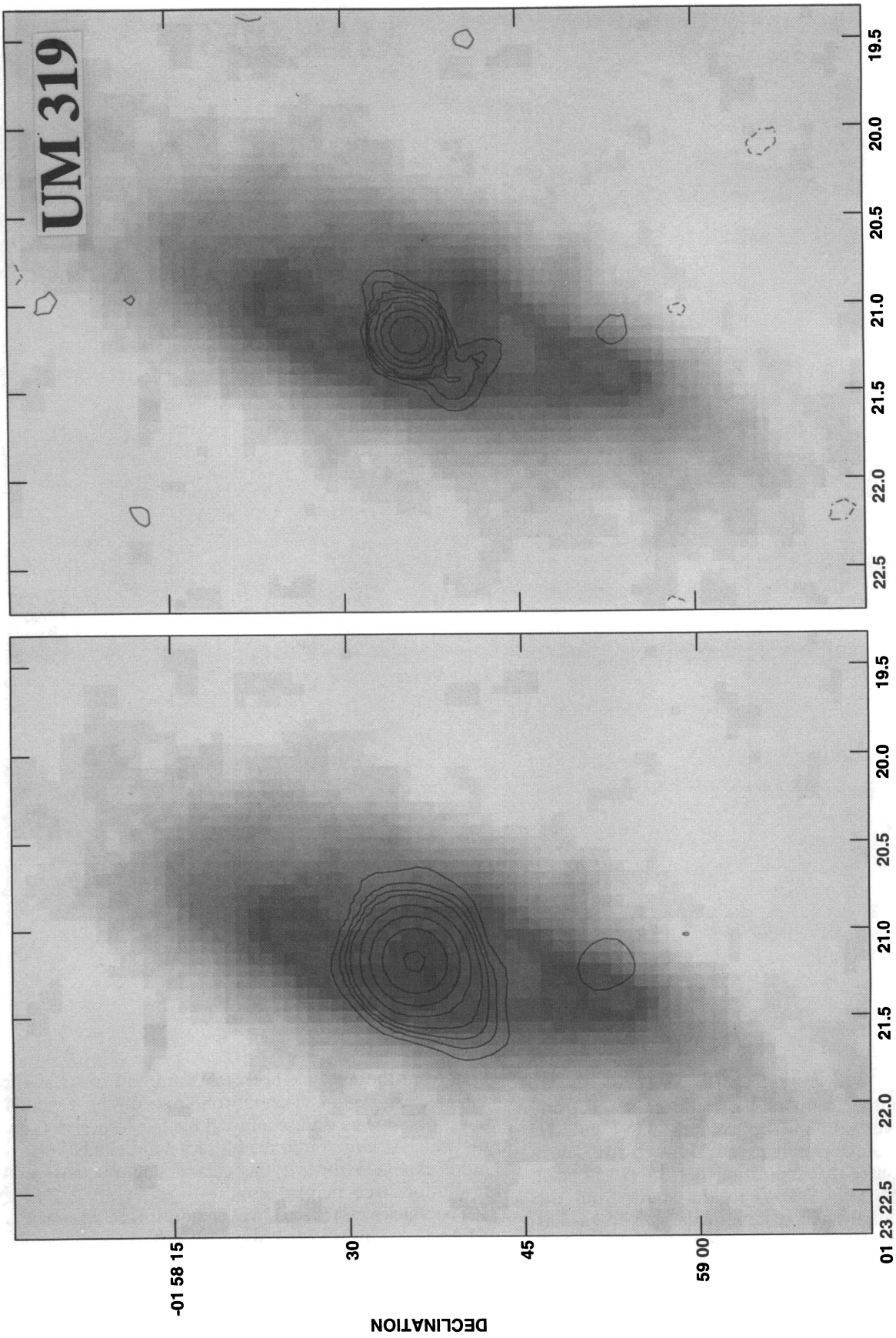

FIG. 1*a*

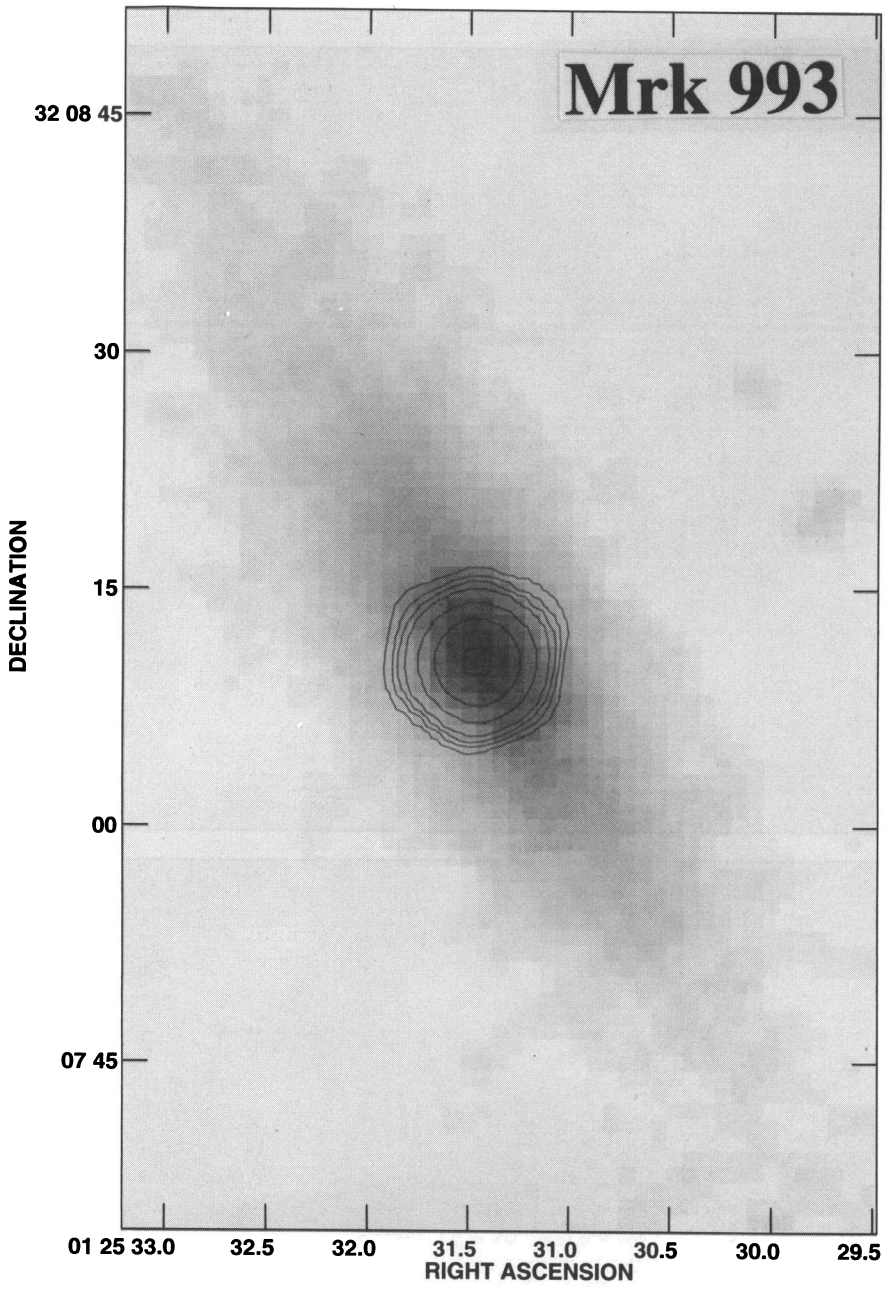

FIG. 1*b*

3.1.10. *MCG −2-27-9*

We show a contour map of the radio emission from MCG −2-27-9 (overlaid on an optical image) in Figure 1*f*. The central radio source is unresolved. However, we detect emission from a source that is positioned ~35″ (10.5 kpc at the distance of MCG −2-27-9) to the south from the nuclear source, along the galaxy minor axis. This source has flux density 0.3 mJy, which corresponds to $P_6 = 1.3 \times 10^{20}$ W Hz^{-1} at the distance of MCG −2-27-9. Follow-up observations would be useful to determine if this source is associated with this galaxy.

3.1.11. *NGC 4235*

In Figure 1*g*, we show contour maps of the radio emission from NGC 4235. Diffuse structures extend out ~1′ (9.3 kpc) from the nucleus, both eastward and westward from the nuclear region. The morphology of the extraplanar emission appears diffuse and bubble-like, especially toward the west. At large radii, the eastern source may be slightly more extended toward the galaxy minor axis (see low-resolution 20 cm map).

The nuclear radio source is unresolved in small-scale VLA maps (Ulvestad & Wilson 1984; Kukula et al. 1995).

3.1.12. *NGC 4388*

We did not obtain new radio images of NGC 4388. Large-scale radio maps (Condon 1987; Hummel et al. 1983) reveal diffuse emission extending out along the minor axis from the nuclear region. In Figure 1*h*, we reproduce a contour map (from Hummel et al. 1983) of the 5 GHz radio

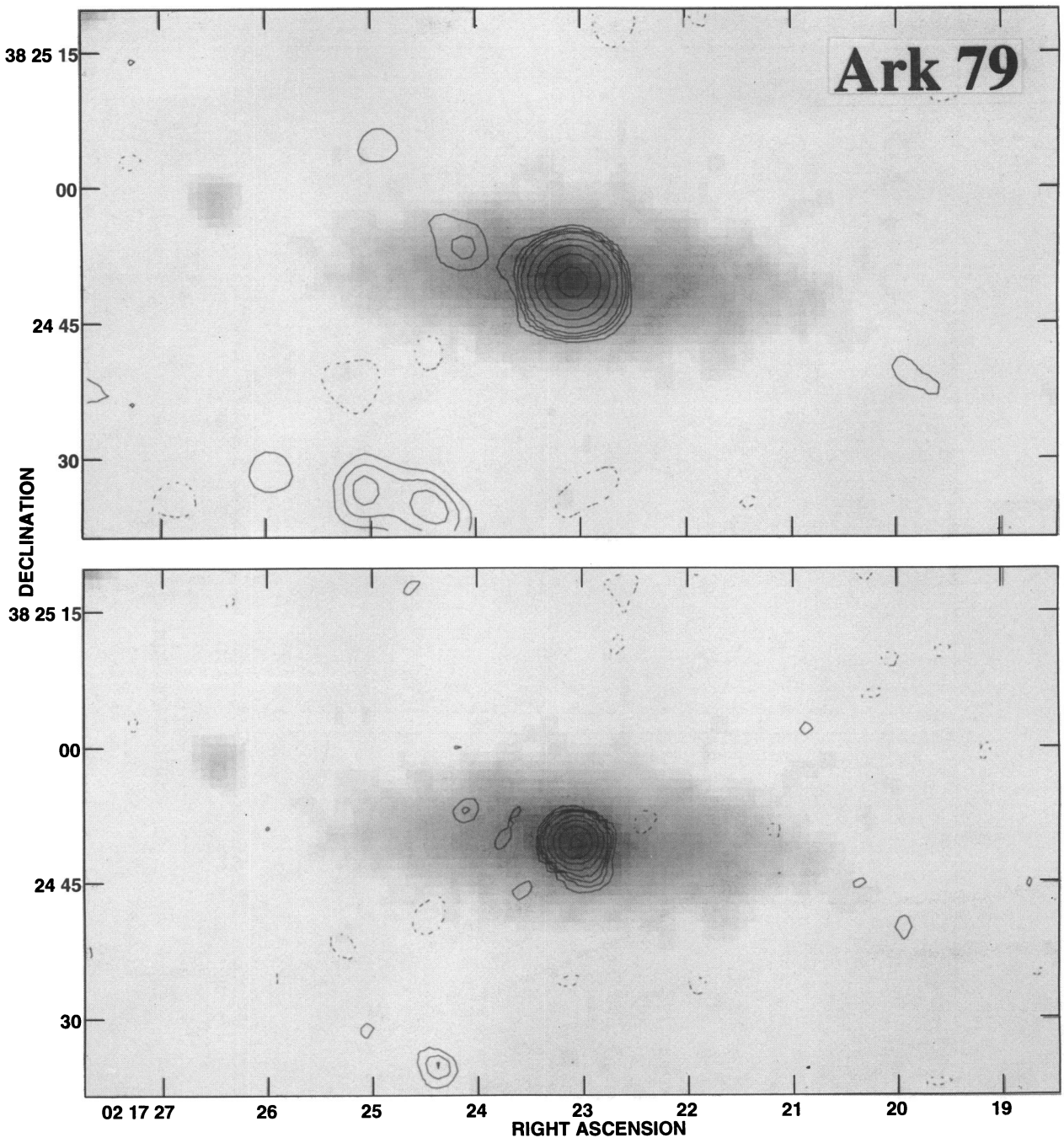

FIG. 1*c*

emission that shows the large-scale radio structures. In a higher resolution radio image by Stone, Wilson & Ward (1988), one can resolve individual "fingers" extending out of the disk into the halo.

3.1.13. *NGC 4602*

We show a contour map of the radio emission from NGC 4602 in Figure 1*i*. The nuclear source is quite weak, and most of the emission comes from sources in the galaxy disk.

3.1.14. *NGC 4945*

The large-scale 4.75 GHz map from Harnett et al. (1989) is reproduced in Figure 1*j*. The extraplanar structure in NGC 4945 extends ~10′ (20 kpc) along the minor axis on both sides of the disk.

3.1.15. *IC 4329A*

We did not obtain new radio images of IC 4329A. As far as we know, the only published radio maps of this galaxy are those in Unger et al. (1987; see Fig. 1*k*). Diffuse radio structure extends westward ~6″ (1.9 kpc) in P.A. ~ 285°, in the general direction of the galaxy minor axis.

3.1.16. *NGC 5506*

We show contour maps of the large-scale radio emission from NGC 5506 in Figure 1*l*. Diffuse, bubble-like radio structures extend out of the disk to radii ~30″ (3.6 kpc) from the nucleus in P.A. ~ 140°. At higher resolution, the nuclear source resolves into a compact core plus diffuse halo (Ulvestad, Wilson, & Sramek 1981; Unger et al. 1986,

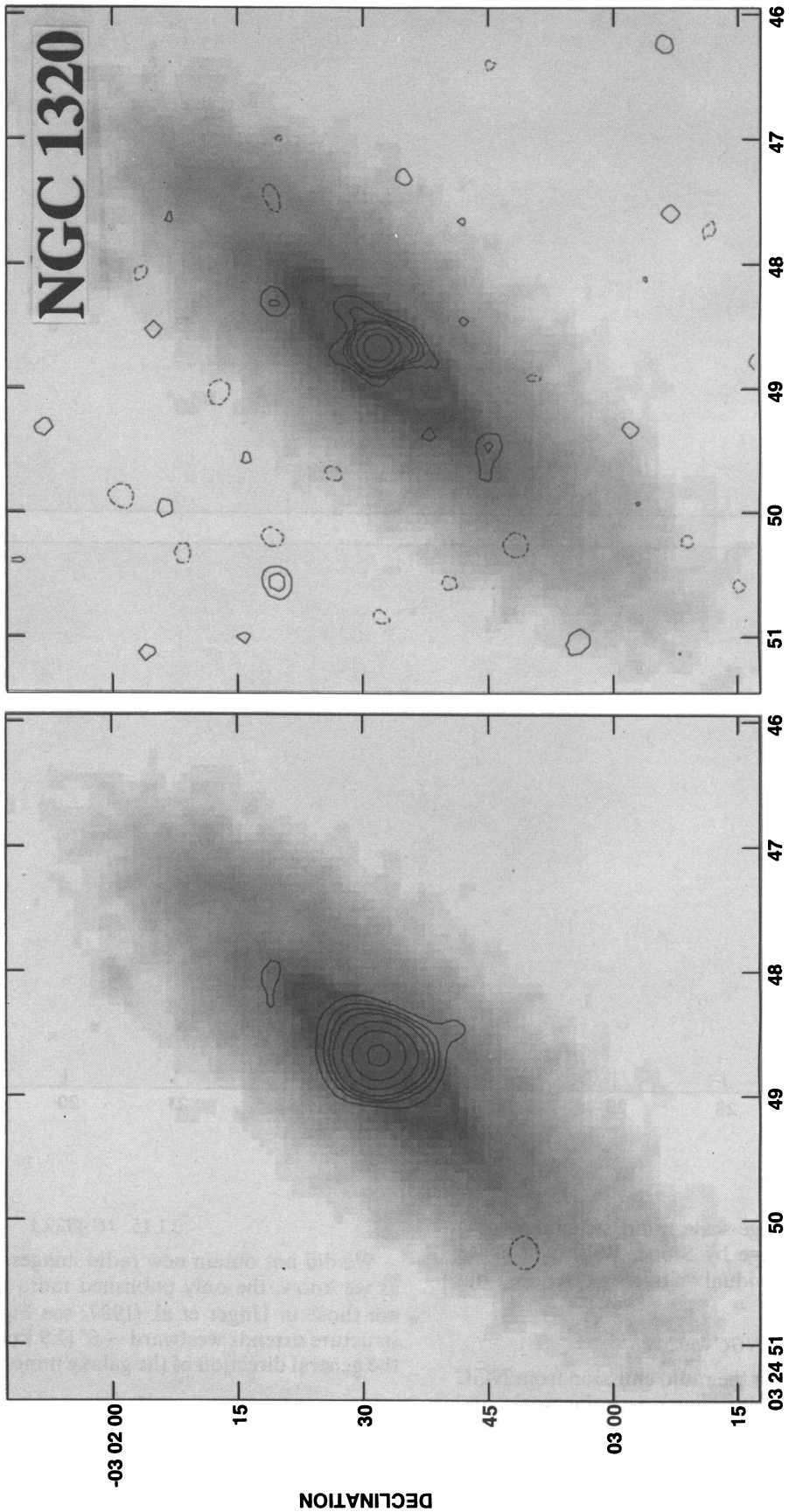

FIG. 1*d*

1987) extending in the same direction as the large-scale "bubbles." Wehrle & Morris (1987) have mapped the small-scale radio halo and have identified a "loop" of diameter ~ 100 pc that originates at the compact source. They attribute this loop to either a bubble of hot plasma rising from the nucleus or a magnetically dominated coronal arch.

3.1.17. *IC 1368*

A contour map of the radio emission is shown in Figure 1*m*. The nuclear source is very slightly resolved in P.A. $\sim 45°$, in the direction of the major axis.

3.1.18. *NGC 7410*

Condon (1987) has published a large-scale 1.5 GHz radio map, which shows a bright, extended radio structure positioned roughly 2'.5 (17.0 kpc) to the northwest, along the minor axis (see Fig. 1*n*). The extended source has a 1.5 GHz flux of 6.3 mJy, which corresponds to a 6 cm radio power $P_6 = 1.7 \times 10^{20}$ W Hz^{-1} (assuming spectral index $\alpha = 0.75$). Its connection with NGC 7410 is speculative, but follow-up studies are warranted to determine if it is associated with this galaxy.

3.1.19. *NGC 7590*

We did not obtain radio images of NGC 7590, and we are not aware of any published radio maps of this galaxy. Wright (1974) quotes a flux density of 70 mJy at 1.4 GHz (and 2.7 GHz) from single-dish observations, and Ward et al. (1980) show that the radio spectrum is quite flat.

3.1.20. *Possible Supernova Remnants or Radio Supernovae in the Disks of Seyfert Galaxies*

Isolated, unresolved radio sources were detected in the disks of the Seyfert galaxies UM 319, Ark 79, NGC 1320, and MCG −2-27-9. Such radio sources may also be present in the disk of the Seyfert galaxy NGC 4602 (see Fig. 1*i*); however, it is difficult to determine from our map if they are individual sources or just localized peaks of diffuse emission from the disk. In Table 3, we list positions, 6 cm fluxes, and 6 cm radio powers for the disk sources in these five galaxies.

Typical radio powers are ~ 1–8×10^{19} W Hz^{-1}, which is at least a factor of 10 larger than the radio power of Cas A (P_6[Cas A] $= 0.8 \times 10^{18}$ W Hz^{-1}). However, the radio powers are comparable to those of radio supernovae (see, e.g., Sramek & Weiler 1990). Follow-up radio studies of all of these galaxies would be useful for determining if the unresolved sources are individual radio supernovae or perhaps groups of SNRs.

TABLE 3

UNRESOLVED RADIO SOURCES IN THE DISKS OF SEYFERT GALAXIES

Galaxy Name	R.A. (J2000)	Decl. (J2000)	F_6[a] (μJy)	P_6[a] (10^{19} W Hz^{-1})
UM 319	01 23 21.2	−01 58 52	126	6.0
Ark 79	02 17 24.1	+38 24 53	135	7.7
NGC 1320	03 24 48.0	−03 02 19	95	1.5
	03 24 49.5	−03 02 46	67	1.0
MCG −2-27-9	10 35 28.0	−14 07 58	105	4.8
	10 35 29.5	−14 07 47	83	3.8
NGC 4602	12 40 33.6	−05 07 46	99	1.4
	12 40 34.2	−05 07 34	331	4.6
	12 40 34.3	−05 07 45	99	1.4
	12 40 35.4	−05 07 47	276	3.8
	12 40 35.9	−05 07 38	292	4.0
	12 40 36.0	−05 07 56	240	3.3
	12 40 36.2	−05 07 39	326	4.5
	12 40 36.8	−05 07 41	235	3.3
	12 40 37.2	−05 07 44	126	1.7
	12 40 37.9	−05 08 07	144	2.0
	12 40 38.1	−05 07 45	457	6.3
	12 40 38.8	−05 08 00	149	2.1
	12 40 39.2	−05 08 12	571	7.9

NOTE.—Units of right ascension are hours, minutes, and seconds, and units of declination are degrees, arcminutes, and arcseconds.

[a] Total flux and power at 6 cm, assuming the source is at the same distance as the galaxy. Fluxes were measured from the normal maps by summing the flux density enclosed in boxes.

3.2. *Individual Objects: Starburst Galaxies*

3.2.1. *UGC 903 (MCG 3-4-26)*

In Figure 2*a*, we show a contour map of the radio emission from UGC 903. Much of the radio emission comes from a disk component. Faint "fingers" appear to extend out of the disk, but it is not clear whether this emission originates from regions above the galaxy plane or is beam-smeared emission from point sources in the disk.

3.2.2. *NGC 1134 (Arp 200)*

A contour map of the radio emission is shown in Figure 2*b*. Nearly all of the emission comes from a boxlike region surrounding the nucleus where massive stars are apparently forming. Such boxy morphology is also present in the 1.5 GHz map from Condon et al. (1990) and the Hα + [N II] image from Lehnert & Heckman (1995).

3.2.3. *NGC 3044*

In Figure 2*c*, we display contour maps of the radio emission from this galaxy. As in the other starburst galaxies in our sample, much of the radio emission from this galaxy comes from the disk component. The disk in NGC 3044 is highly inclined, and it is easy to confirm the presence of a radio halo extending above the disk (e.g., see our tapered image). This radio halo has been previously noted by Hummel & van der Hulst (1989). The 1.5 GHz map from Condon et al. (1990, reproduced in Fig. 2*c*) clearly shows emission from this radio halo.

3.2.4. *NGC 7541*

We show a contour map of the radio emission overlaid on an optical image in Figure 2*d*. Again, most of the emission comes from sources in the disk, especially from regions along the eastern arm. As in UGC 903, "fingers" seem to extend out of the disk, but this may be beam-smeared emission from point sources in the disk.

3.3. *Properties of the Large-Scale Radio Sources*

3.3.1. *Radio Fluxes and Powers*

For each of the 14 galaxies we observed, we list the total 4.9 GHz radio flux (F_T) in Table 4, column (2) (corresponding total radio powers are listed in Table 1). Total fluxes were measured (using the normal maps) by summing the flux density inside boxes enclosing all of the emission from the galaxy. We also list nuclear fluxes F_N (peak flux density in the nuclear region in the hi-res maps) and corresponding nuclear powers P_N (Table 4, cols. [3] and [4], respectively).

One would like to separate the radio emission produced by the outflow from that produced by the rest of the galaxy. In order to achieve this, we first calculated an "extranuclear" radio power P_{XN} (Table 4, col. [5]) from the extranuclear flux $F_{XN} = F_T - F_N$. We then corrected P_{XN}

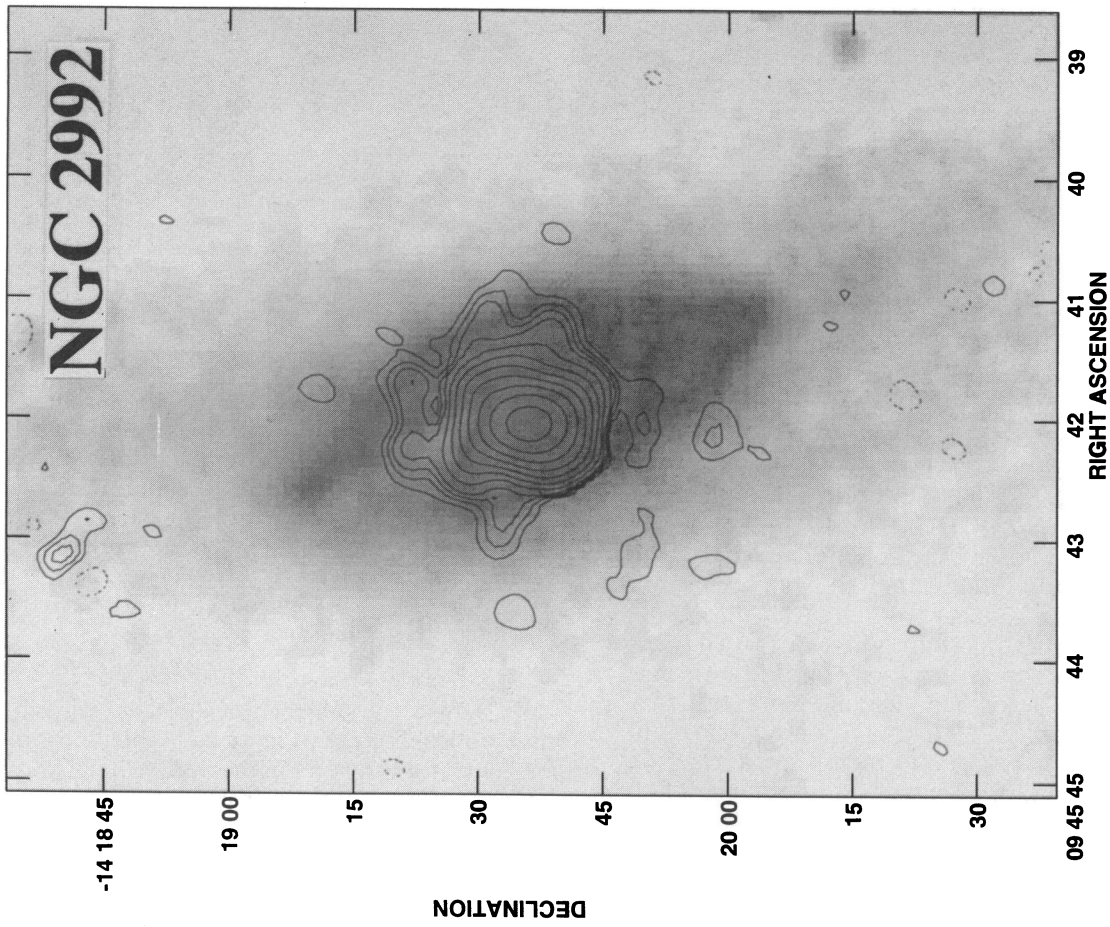

FIG. 1*e*

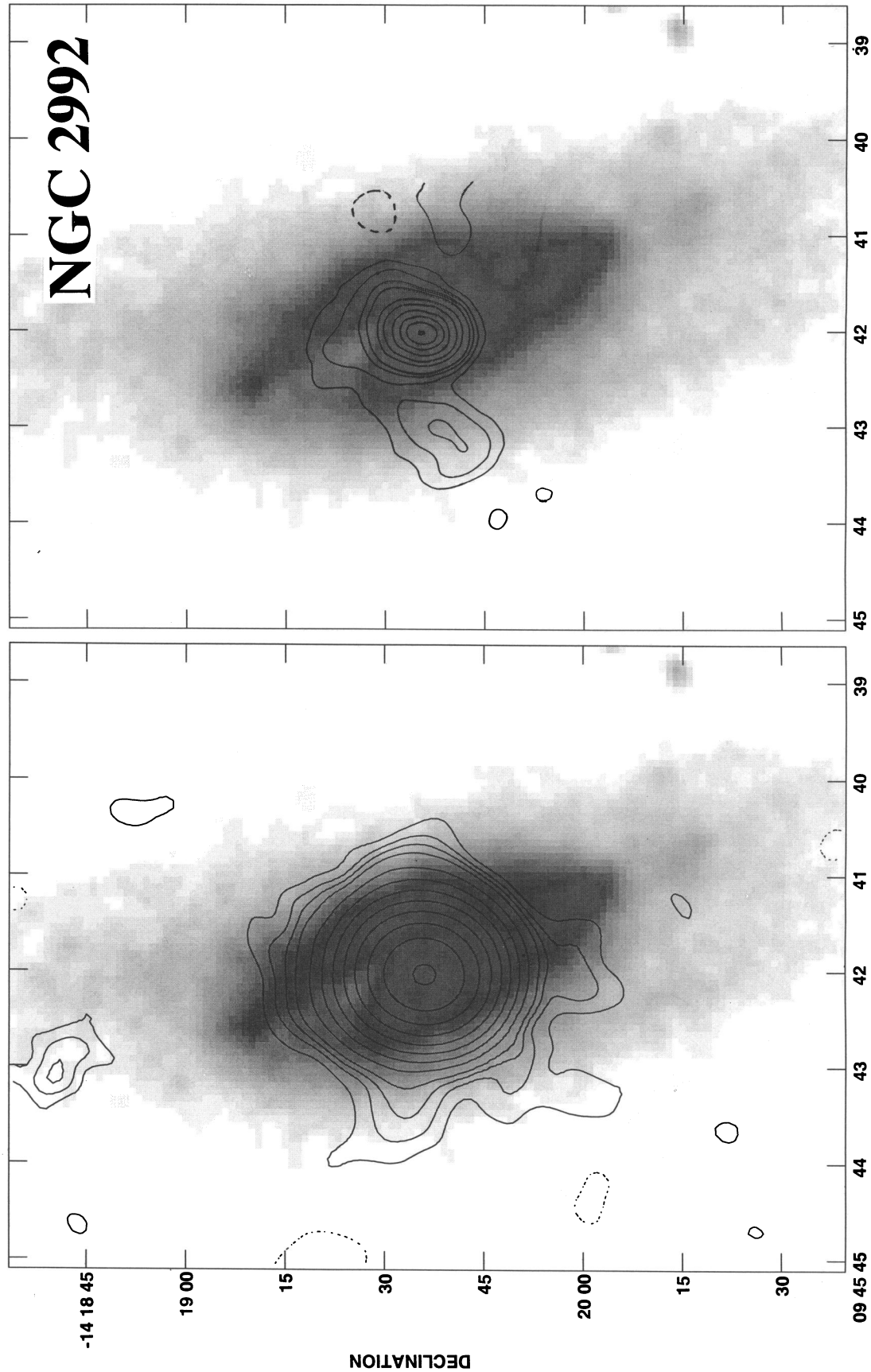

FIG. 1e—*Continued*

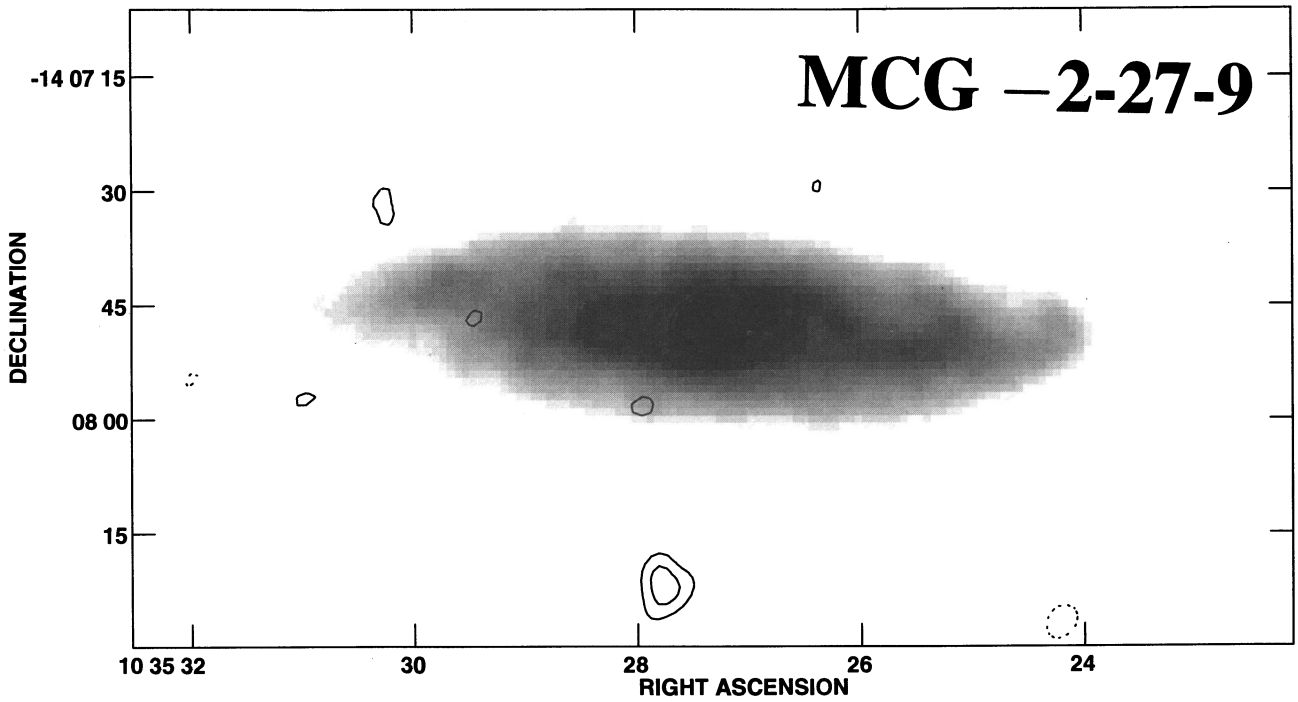

FIG. 1*f*

by subtracting radio powers of sources that were clearly associated with disk emission (see, e.g., Table 3). In most cases, the total radio power from individual sources in the disk is much smaller than that from the LSO. These "corrected" extranuclear powers are good estimates of the radio power from the LSOs, so we denote them as P_{LSO} in Table 4 (col. [6]).

This method worked quite well for most of the Seyfert galaxies since their disk sources are, in general, isolated from the nuclear radio sources. In three Seyferts (Mrk 993, MCG −2-27-9, and IC 1368), the extranuclear emission is not well imaged in our maps and we do not list values for P_{LSO}. In the four starburst galaxies and in the Seyfert galaxy NGC 4602, the disk emission is not easy to distinguish from possible extraplanar emission. Although extraplanar radio emission is clearly present in the starburst galaxy NGC 3044, estimating the radio power of this component is not straightforward. An accurate estimate would involve suc-

TABLE 4

NUCLEAR AND EXTRANUCLEAR RADIO COMPONENTS

Galaxy Name (1)	F_T[a] (mJy) (2)	F_N[a] (mJy) (3)	P_N[b] (log W Hz^{-1}) (4)	P_{XN}[c] (log W Hz^{-1}) (5)	P_{LSO}[d] (log W Hz^{-1}) (6)	μ_{XN}[e] (7)	Notes[f] (8)
UM 319	5.7	4.0	21.28	20.92	20.9	3.00	lin struct, src in disk
Mrk 993	2.3	1.9	20.95	20.30	...	...	unr or v sl res
Ark 79	6.2	4.4	21.40	21.01	21.0	...	sl res to SW, src in disk
NGC 1320.....	3.5	2.1	20.51	20.35	20.3	3.24	lin struct, srcs in disk
NGC 2992.....	87.7	37.8	21.63	21.76	21.8	2.29	lots of struct, extent min axis
MCG −2-27-9.....	1.0	0.6	20.40	20.29	...	...	extent to SE, srcs in disk
NGC 4235.....	8.6	4.6	20.75	20.70	20.7	1.89	unr, v extended
NGC 4602.....	6.1	1.9	20.42	20.76	...	...	weak nuc src, clumpy disk
NGC 5506.....	178.8	139.2	21.99	21.44	21.4	2.37	lots of struct, extent min axis
IC 1368	10.4	8.9	21.46	20.70	...	...	sl res along maj axis
UGC 903	19.7	4.0	20.73	21.32	...	...	clumpy disk, fingers out of disk
NGC 1134.....	27.9	4.0	21.05	21.83	...	...	clumpy disk
NGC 3044.....	37.0	1.9	19.84	21.10	19.7	...	clumpy disk, halo
NGC 7541.....	58.5	10.5	21.21	21.87	...	...	clumpy disk, fingers

NOTE.—The 10 edge-on Seyfert galaxies are listed first, and the four starburst galaxies are listed next.

[a] 6 cm fluxes. Total flux from the galaxy F_T was measured by summing the flux density inside a box enclosing all of the emission from the galaxy. Nuclear flux F_N was estimated from the peak flux density in the nuclear region, using the "hi-res" maps (see § 2).

[b] Nuclear 6 cm radio powers, calculated from F_N.

[c] Extranuclear (XN) 6 cm radio powers. The extranuclear power P_{XN} was calculated directly from $F_{XN} = F_T - F_N$.

[d] The extranuclear 6 cm radio powers associated with the large-scale outflows (LSOs). Except for NGC 3044, P_{LSO} was calculated by subtracting contributions from sources in the disk from P_{XN}. For NGC 3044, flux of the radio halo (roughly estimated from Fig. 2*c*) was used to calculate P_{LSO}.

[e] Logarithm of ratio of 60 μm flux density to extranuclear 6 cm flux density F_{XN}.

[f] Notes about radio structure. For the Seyfert galaxies, the nuclear structure is first described and then the extranuclear structure. Abbreviations: lin = linear, struct = structure, src = source, min = minor, unr = unresolved, v = very, nuc = nuclear, sl = slight(ly), res = resolved, maj = major.

cessfully modeling the radio morphology of the disk component. We estimate a rough extraplanar flux of 0.3 mJy (from Fig. 2*c*), which corresponds to a 4.9 GHz radio power of $10^{19.7}$ W Hz^{-1} ($\sim 10^{-1.4}$ of the total 6 cm radio power). Thus, we were able to measure $P_{\rm LSO}$ for six of our Seyfert galaxies and one of our starburst galaxies.

3.3.2. *Intrinsic Properties*

For the six Seyfert galaxies in Table 4 with large-scale radio structures, we estimated maximum lifetimes (see van der Laan & Perola 1969) of the cosmic rays producing the synchrotron radiation. Equipartition between magnetic field and particle energy was assumed, and the radio sources were assumed to have cylindrical geometry. Magnetic pressures in the radio sources are ~ 0.5–10×10^{-14} ergs cm^{-3} and total energies (in particles and magnetic field) are ~ 0.1–2×10^{53} ergs. By dividing the lifetimes (typically 1–2×10^7 yr) of the synchrotron-emitting electrons by the radial extent of the sources (Table 5), we estimate *minimum* outflow velocities of ~ 50–100 km s^{-1} for UM 319, Ark 79, NGC 1320, NGC 2992, and NGC 5506 and ~ 450 km s^{-1} for NGC 4235. Thus, near-relativistic outflows are not required.

3.3.3. *Radial Extent from Nucleus and Orientation*

Geometrical properties were measured for the large-scale radio sources in nine of the 22 Seyfert galaxies in our complete sample. Other than the six Seyferts discussed in the previous section, three more galaxies in our complete sample (NGC 4388, NGC 4945, and IC 4329A, which we did not observe) have large-scale radio structures. Although NGC 7410 and MCG −2-27-9 both have radio sources that are positioned along their minor axes, more evidence is needed to show that the sources are associated with these galaxies. In Table 5, for each of these nine galaxies, we list position angle (P.A.) with respect to the nucleus; maximum projected radius from the nucleus; P.A. of the major axis of the galactic disk; and Δ, the difference in angle between the P.A. of the radio source and that of the major axis.

4. DISCUSSION

4.1. *The Nature of Large-Scale Radio Emission in Seyfert Galaxies*

4.1.1. *Frequency of Occurrence*

Large-scale radio structures seem to be a fairly common feature of Seyfert galaxies. In six of the 10 Seyferts we observed, large-scale radio sources clearly extend out of the nuclear region (i.e., radii $\gtrsim 1$ kpc). Therefore, such large-scale radio structures are likely to be present in $\gtrsim \frac{1}{2}$ of all Seyferts. Suitable radio maps are not available for many of the remaining 12 objects in our complete sample, but such large-scale radio emission is clearly present in at least three of these 12 galaxies.

In comparison, in starburst galaxies, large-scale radio emission at these surface brightness levels is probably less common. Although our detection frequency of $\frac{1}{4}$ is consistent with an inherent frequency of occurrence of 50%, in larger surveys of edge-on galaxies, only a few percent of edge-on galaxies show signs of radio halos (see, e.g., Hummel, Beck, & Dettmar 1991).

4.1.2. *Radio Powers*

The 6 cm radio powers $P_{\rm LSO}$ of the large-scale radio sources in the Seyferts are $\sim 10^{20}$–10^{22} W Hz^{-1} (Table 4), which are at least several orders of magnitude weaker than radio powers of lobes in typical FR II radio galaxies. It is also noteworthy that, while in radio galaxies core powers are weaker than lobe powers (see, e.g., Zirbel & Baum 1995), in Seyferts, the nuclear powers P_N are typically larger than $P_{\rm LSO}$ (Table 4; see also Baum et al. 1993).

Measurements of radio powers of halos in starburst galaxies are not widely available because of the difficulty of separating emission from the disk. Our estimate of the radio power of the halo in NGC 3044 is $\sim 10^{19.7}$ W Hz^{-1} (§ 3.3), roughly consistent with the range of $P_{\rm LSO}$ for our Seyferts.

4.1.3. *Radial Extent from Nucleus*

In Figure 3, we show a histogram of the maximum projected radius of the large-scale radio emission in the Sey-

TABLE 5

GEOMETRICAL PROPERTIES OF LARGE-SCALE RADIO EMISSION IN SEYFERT GALAXIES

GALAXY NAME (1)	P.A. (LSO)[a] (deg) (2)	MAX RADIUS[b] (arcsec) (3)	MAX RADIUS[b] (kpc) (4)	REFERENCES[c] (5)	P.A. (MAJ)[d] (deg) (6)	Δ[e] (deg) (7)
UM 319	130	10	3.2	1	165	35
Ark 79	200	6	1.9	2	87	67
NGC 1320.....	180	6	1.1	2	135	45
NGC 2992.....	105	25	3.7	3	15	90
NGC 4235.....	275	62	9.7	4	48	47
NGC 4388.....	0	22	3.6	3	92	88
NGC 4945.....	140	960	31.4	5	43	83
IC 4329A	285	6	1.9	6	45	60
NGC 5506.....	145	38	4.4	4	91	54

[a] Position angle of large-scale radio structure.

[b] Maximum projected radius of large-scale radio emission along P.A. listed in col. (2).

[c] References for maps used to measure P.A. (col. [2]) and projected radius (cols. [3] and [4]).—(1) This paper, normal map; (2) this paper, hi-res map; (3) Hummel et al. 1983—see Figs. 1*e* and 1*h*; (4) this paper, tapered map; (5) Harnett et al. 1989—see Fig. 1*j*; (6) Unger et al. 1987—see Fig. 1*k*.

[d] Position angle of the major axis of the galaxy, taken from RC3 or measured from the digitized optical sky survey plates.

[e] Difference in angle between galaxy major axis and P.A. of large-scale radio emission.

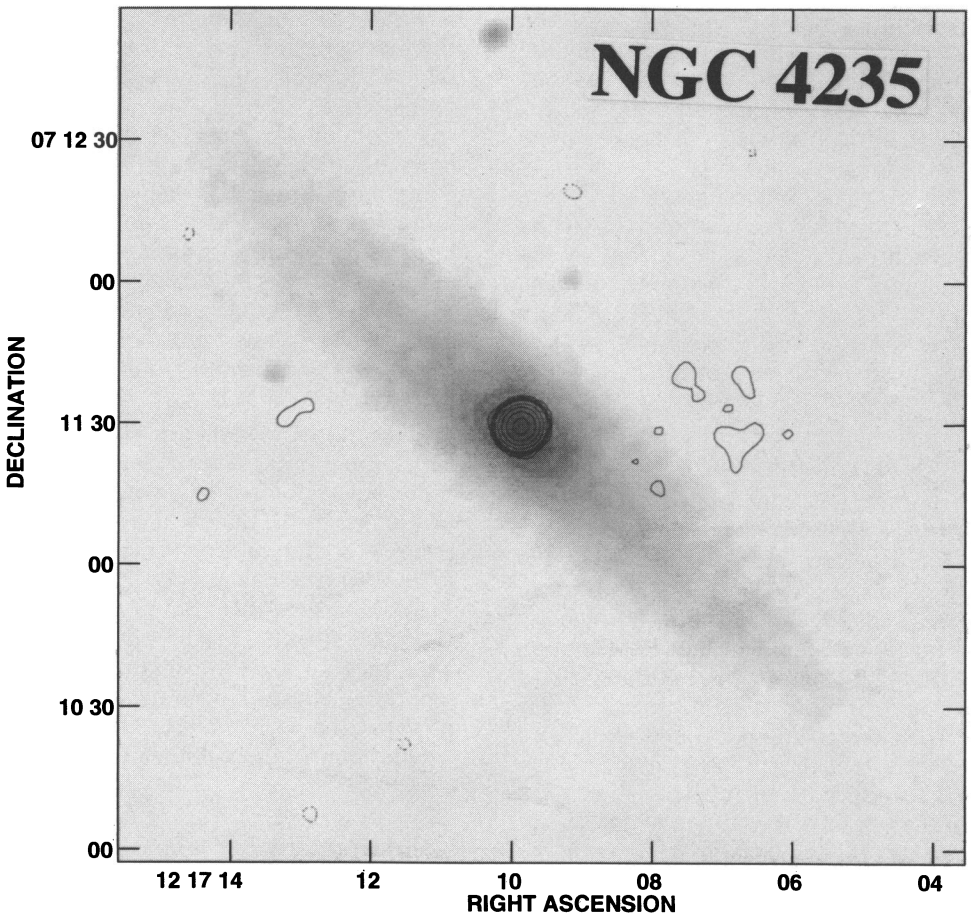

FIG. 1*g*

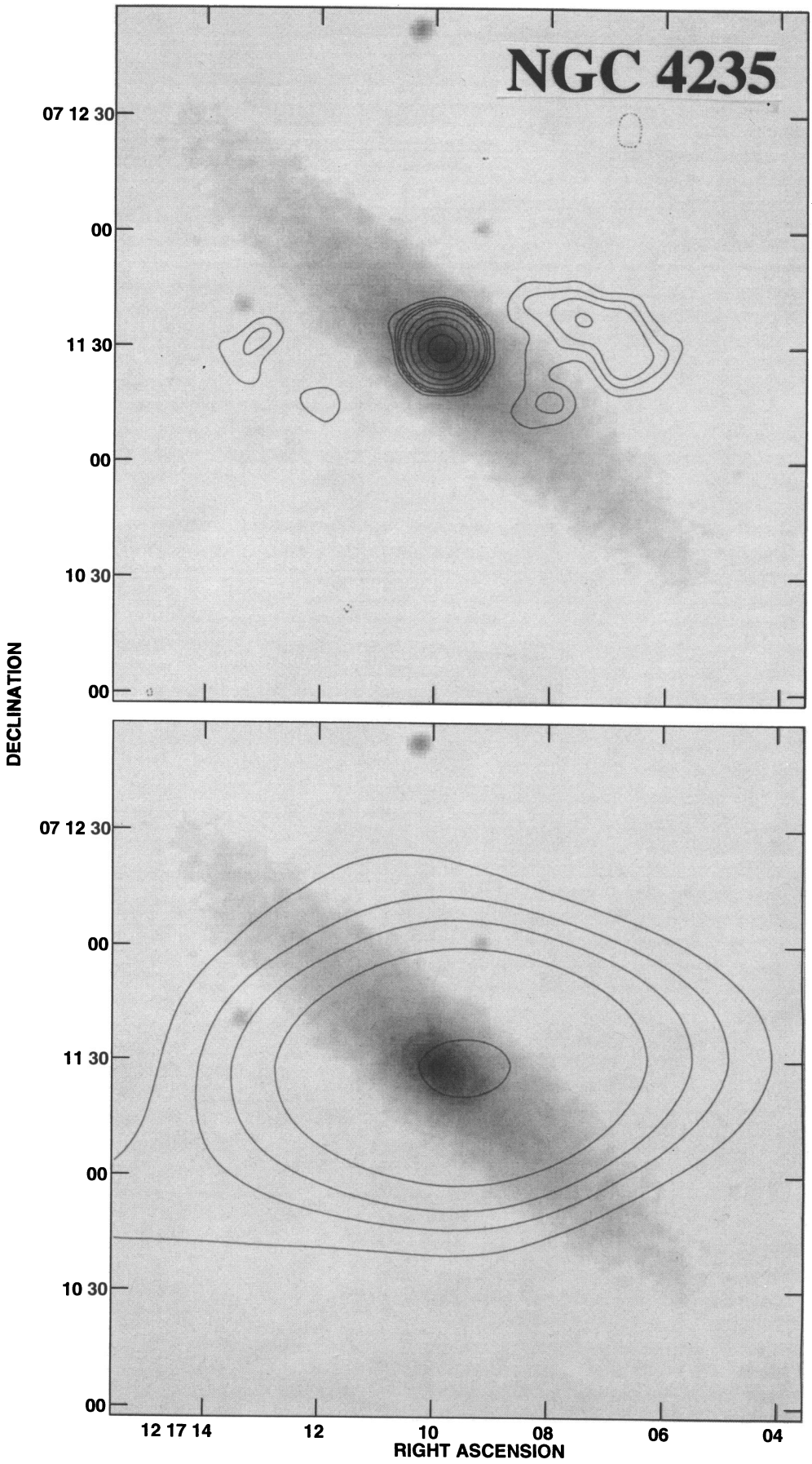

FIG. 1*g*—*Continued*

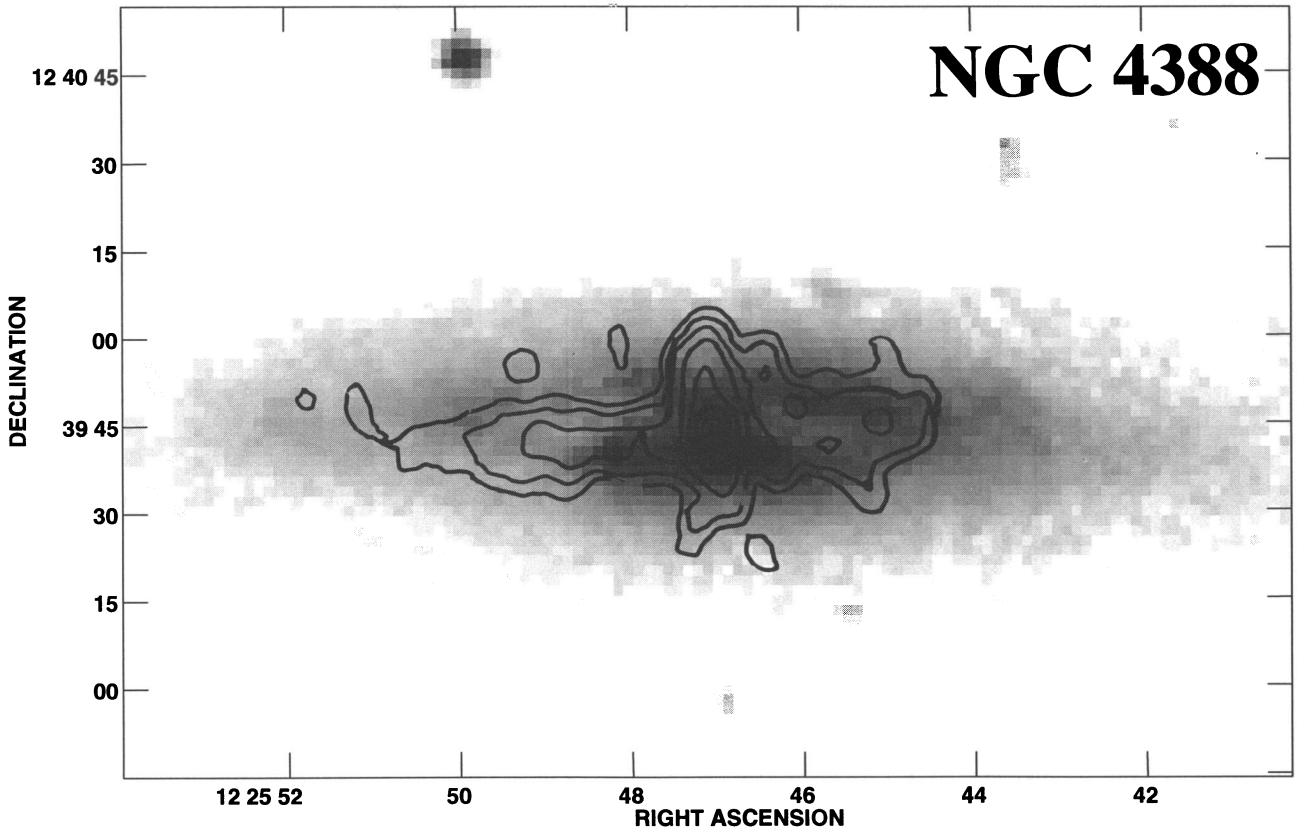

FIG. 1*h*

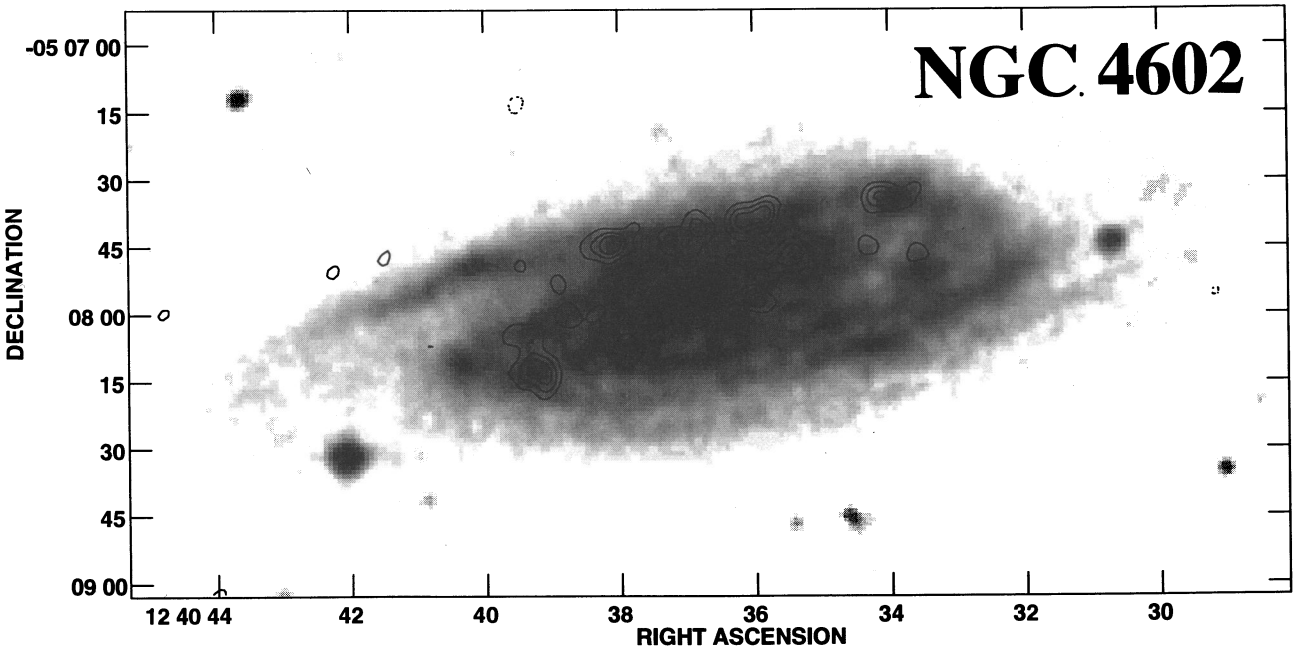

FIG. 1*i*

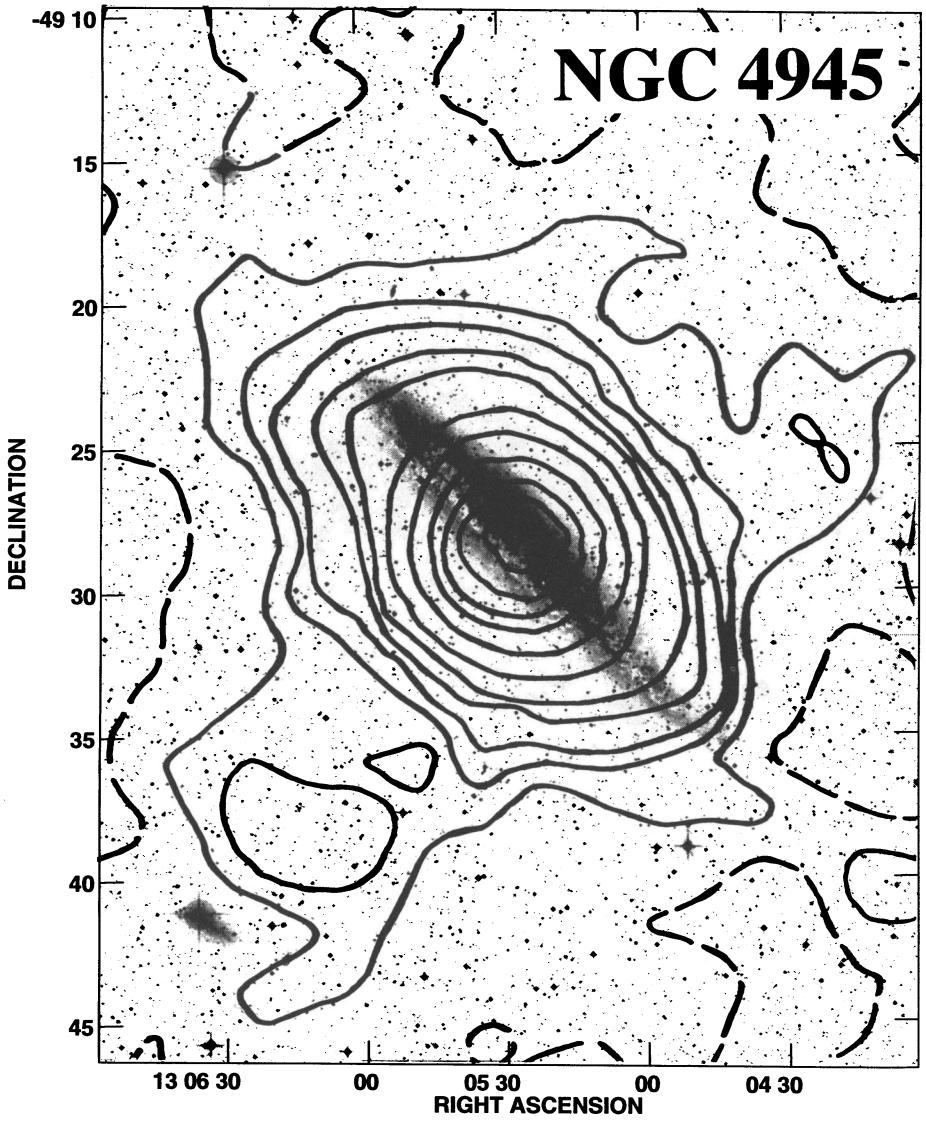

FIG. 1*j*

ferts. Typical radii are 1–5 kpc, although large-scale structures extend out to ~10 and ~30 kpc in NGC 4235 and NGC 4945, respectively. Typical sizes for lobes in radio galaxies are larger, up to $\sim 10^2$–10^3 kpc. Radial extents of radio halos in starburst galaxies are more typical of what is found for large-scale sources in Seyferts. For example, the radial extent of the radio halo in NGC 3044 is ~2.5 kpc (Fig. 2*c*). More prominent halos, such as those in NGC 253 (Carilli et al. 1992), M82 (Seaquist & Odegard 1991), and NGC 4631 (see Dahlem, Lisenfeld, & Golla 1995), extend out to radii of several tens of kpc.

4.1.4. *Morphology*

Although large-scale radio sources in Seyferts are similar in radio power and radial extent to those in starburst galaxies, their radio morphologies do not typically resemble spherical halos. An exception is the extended radio source in the Seyfert galaxy NGC 4945 (Fig. 1*j*). According to Heckman, Armus, & Miley (1990), a starburst-driven superwind is present in this galaxy, and so, in this case, the radio halo may be produced by this superwind. In general, large-scale radio sources in Seyferts are diffuse structures originating from a small region surrounding the nucleus. In some objects, such as UM 319 and NGC 1320, the structures have linear morphologies which resemble collimated outflows. Others, such as NGC 4235, have bubble-like radio structures.

4.1.5. *Orientation*

At what angle do the radio sources emerge from the galaxy disk? In Figure 4, we plot a histogram of Δ (Table 5, col. [7]), the difference between the P.A. associated with the extended radio emission (Table 5, col. [2]) and the P.A. of the galaxy major axis (Table 5, col. [6]). Radio halos in edge-on starburst galaxies are typically oriented perpendicular to the galaxy major axes. Therefore, if LSOs in Seyfert galaxies are wide-angled winds blowing out perpendicular to the galaxy disk, one might expect the distribution in Δ to be peaked near 90°. If, on the other hand, the LSOs are jets that are oriented isotropically, the distribution in Δ is expected to be flat. The observed distribution in Δ (Fig. 4) is consistent with directed outflows (e.g., jets) that, for some reason, do not extend to kiloparsec scales when they are oriented with the plane of the galaxy disk (Δ ~ 0°) but are otherwise oriented isotropically.

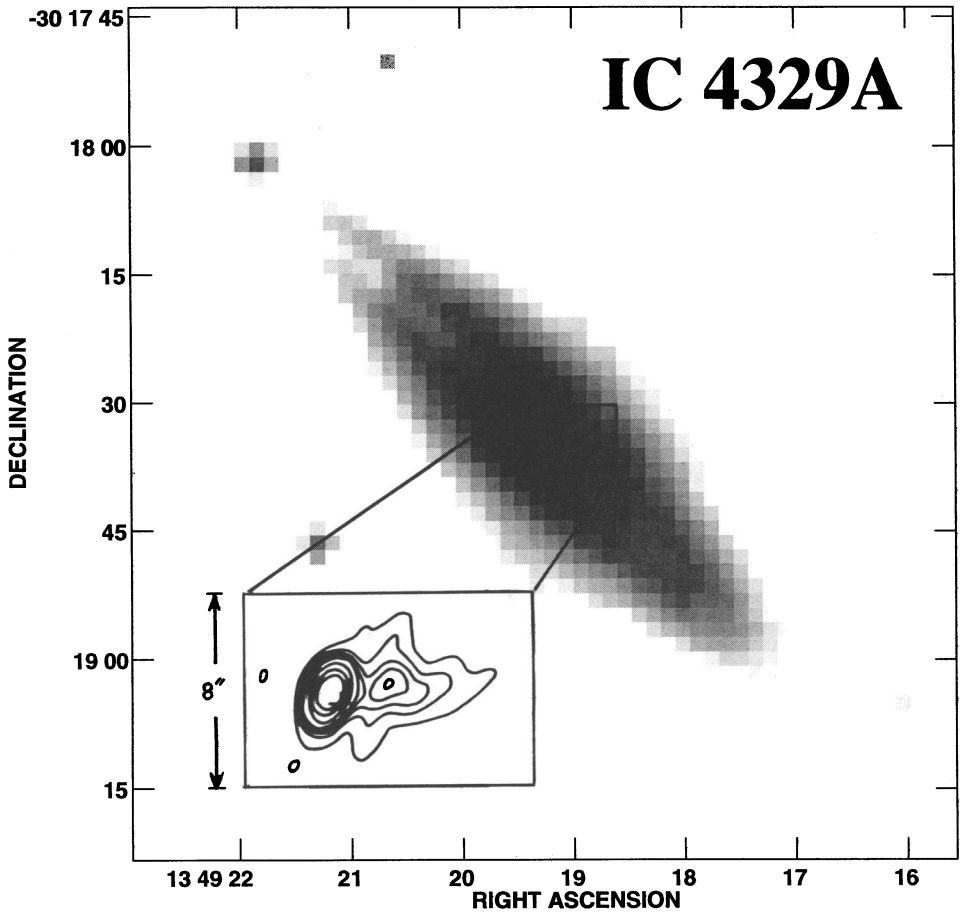

FIG. 1*k*

Baum et al. (1993) found that the extranuclear sources in their sample were preferentially oriented perpendicular to the major axes ($\Delta \gtrsim 60°$). Many of the galaxies in the sample of Baum et al. were relatively face-on, which can give rise to misleading results for the following two reasons. First, the P.A. of the major axis is difficult to determine and thus has larger uncertainty. Second, in face-on galaxies, the relationship between Δ and the angle between the radio source and the plane of the galaxy disk is more ambiguous. Thus, the results from our sample of edge-on Seyferts may be more accurate. However, another consideration is that, as previously noted, the galaxies in the sample of Baum et al. have larger total radio power than those in our sample. More powerful outflows will more easily penetrate the galaxy disk and extend to larger radii. Thus, they may be more easily influenced by global forces from the galaxy (i.e., buoyancy forces) than are weaker outflows which do not escape from the nuclear region.

4.1.6. *Associated Optical Emission*

In Paper I, we presented Hα + [N II] images and optical long-slit spectra of 22 edge-on Seyfert galaxies and used these data and other published data to search for evidence for LSOs. Our results implied that LSOs are present in $\gtrsim \frac{1}{4}$ of all Seyfert galaxies. From our new radio data, we find that large-scale radio emission in Seyfert galaxies is even more common (present in $\gtrsim \frac{1}{2}$ of objects observed).

In Table 6, we list all objects in our complete sample of Seyfert galaxies that have evidence for an outflow from either optical or radio observations. Ten of 22 galaxies are listed, consistent with LSOs being present in $\gtrsim \frac{1}{2}$ of all Seyferts. Extraplanar radio emission and minor axis optical emission-line regions are fairly common, but obviously the presence of one does not always imply the presence of the other. Optical line emission produced by shocks in super-

TABLE 6

EVIDENCE FOR LARGE-SCALE OUTFLOWS IN EDGE-ON SEYFERT GALAXIES

Galaxy Name	Optical Evidence[a]	Radio Evidence[b]
UM 319	...	XN
Ark 79	S?	XN
NGC 1320.....	None	XN
NGC 2992.....	I	XP
NGC 4235.....	None	XP
NGC 4388.....	I, S	XN
NGC 4945.....	I, S	XP
IC 4329A	I	XN
NGC 5506.....	I, S	XP
IC 1368	I	None

[a] Evidence for minor axis outflows from Paper I. Three ellipsis dots denote insufficient data, whereas "none" denotes no evidence. "I" denotes evidence from Hα + [N II] images, and "S" denotes evidence from long-slit spectra. Question mark indicates only suggestive evidence.

[b] Evidence for large-scale outflows from the present radio maps. "XN" denotes large-scale ($\gtrsim$1 kpc) extranuclear radio emission, "XP" (for extra planar) denotes that emission clearly extends out of the optical disk of the galaxy (see Fig. 1), and "none" denotes no evidence.

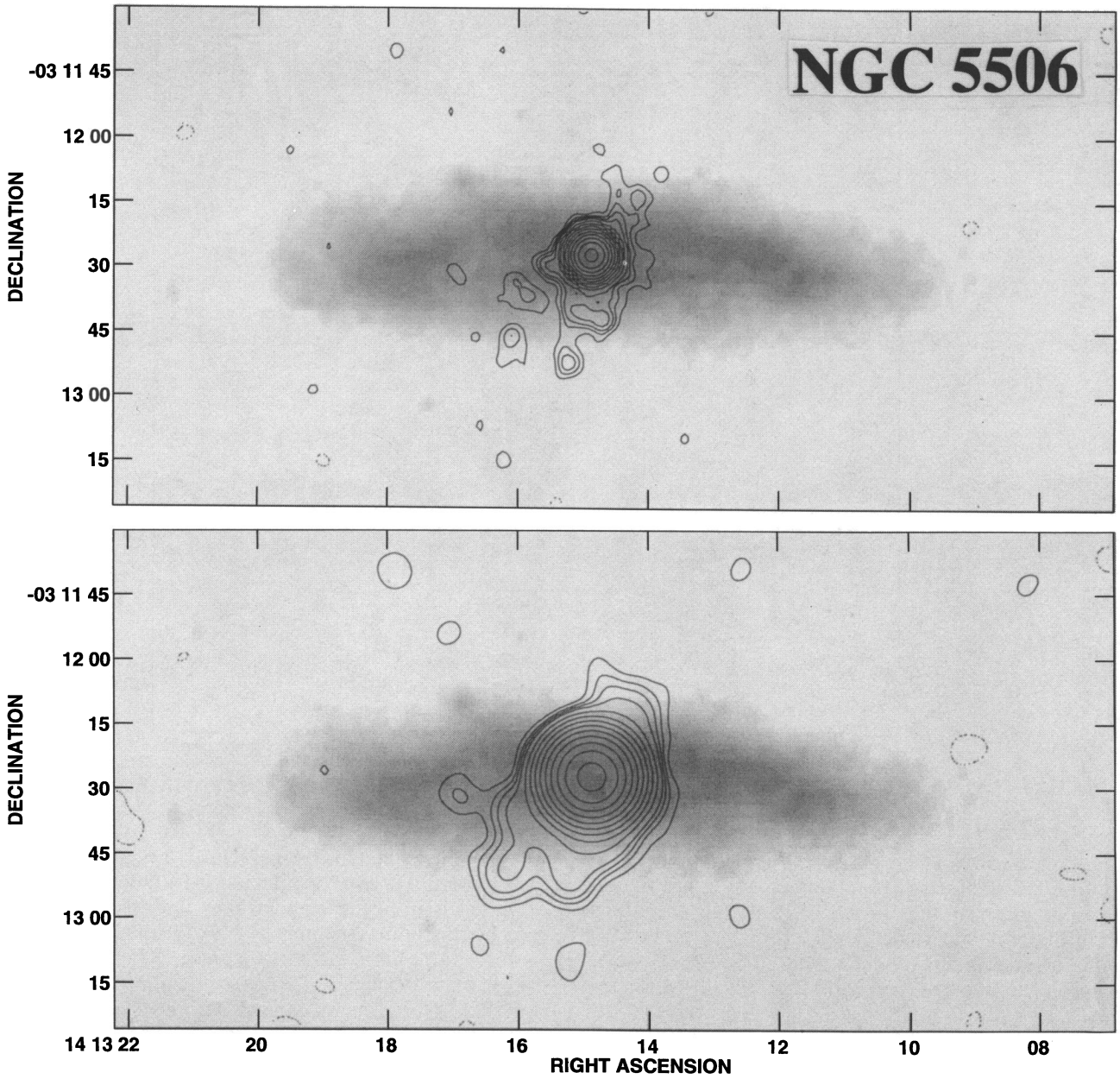

FIG. 1*l*

winds typically has low surface brightness (10^{-17} ergs s^{-1} cm^{-2} arcsec^{-2} or lower; see, e.g., Heckman et al. 1990) and could easily have been present but below our detection limits. On the other hand, some of the optical line emission could be photoionized by the AGN, in which case it may not be cospatial with radio emission produced by the outflow, if such radio emission is present.

Of the nine galaxies with large-scale radio sources, five (NGC 2992, NGC 4388, NGC 4945, IC 4329A, and NGC 5506) also show strong optical evidence for an outflow. These five galaxies also show kinematically disturbed (double-peaked and complex line profiles) and high-velocity gas along their minor axes (Tsvetanov, Dopita, & Allen 1996; Corbin, Baldwin, & Wilson 1988; Heckman et al. 1990; Wilson & Penston 1979 [nuclear spectra only]; Wilson, Baldwin, & Ulvestad 1985, respectively).

An interesting case in which we did not find associated optical line emission is that of NGC 4235. Radio emission clearly extends along the minor axis, on both sides of the galaxy plane (Fig. 1*g*), but extended optical line emission is present along the *major* axis of the galaxy (Paper I; Pogge 1989).

Conversely, some objects show extended optical emission-line gas along their minor axis without associated radio emission. For example, in Paper I, we showed that in IC 1368, a bisymmetric emission-line halo extends along the minor axis, but our radio maps do not show any extra-planar radio emission extending in that direction (see Fig. 1*m*).

4.1.7. *Summary of Properties*

In summary, large-scale ($\gtrsim$1 kpc) radio sources in Seyferts (1) are quite common (present $\gtrsim\frac{1}{2}$ of the time); (2) typically have 4.9 GHz radio powers $\sim 10^{20}$–10^{22} W Hz^{-1}, lower than that of jets and lobes in radio galaxies, but approximately the same as that of radio halos in starburst

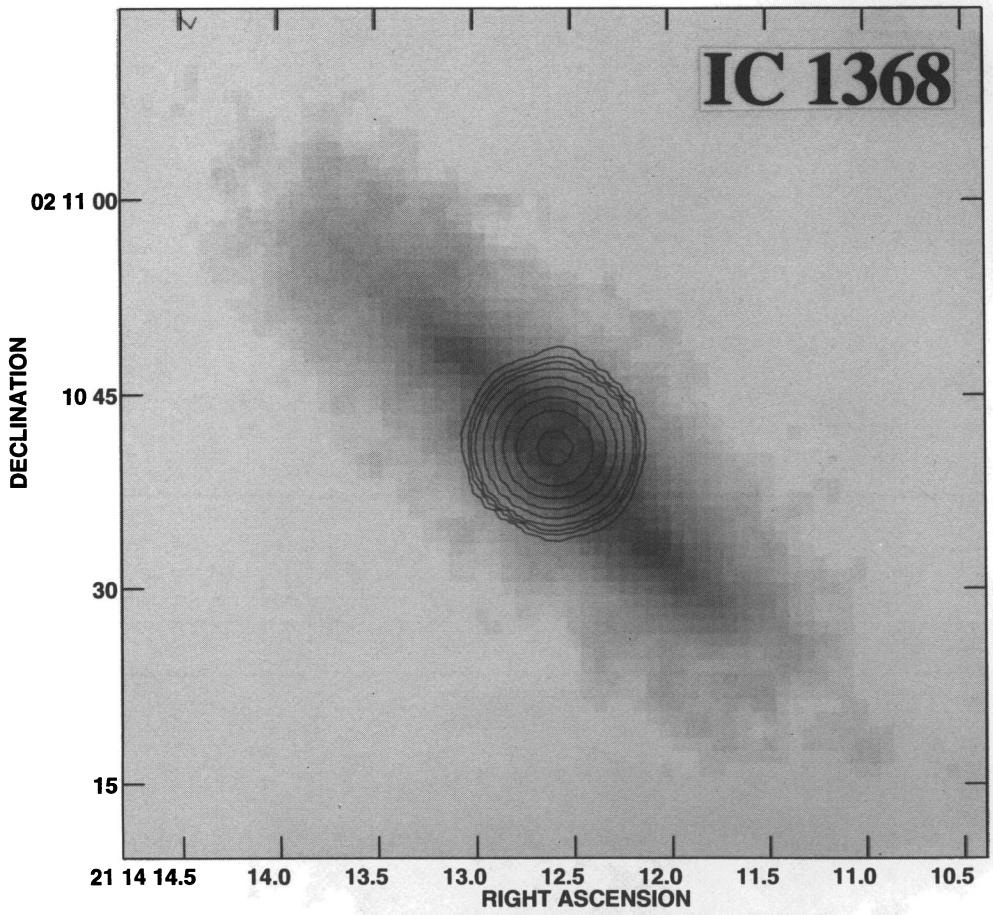

FIG. 1*m*

galaxies; (3) typically extend out to radii of ~1–5 kpc; (4) have diffuse morphologies resembling emission from collimated outflows from the nuclear region; (5) appear to emerge from the disk at angles ~40–90° with respect to the galaxy major axes; and (6) are often (but not always) associated with optical line emission and kinematically disturbed gas.

4.2. *The Origin of Large-Scale Radio Emission in Seyfert Galaxies*

Since we have established that large-scale ($\gtrsim$1 kpc) radio sources are fairly common in Seyferts, it is important to determine how they are produced. A natural explanation is that the Seyfert nucleus both produces the relativistic plasma and powers the outflow, perhaps in a "jet" analogous to those found in classical radio galaxies and radio-loud quasars. The jet would then interact with the galactic medium, shocking clouds of gas and entraining gas as it moves outward, producing associated optical and X-ray emission. However, relativistic plasma can also be produced by star formation activity (e.g., SNRs) in the nuclear region, and, if a strong circumnuclear starburst is present, it could also provide energy for driving an outflow out of the nuclear region. Thus, two central questions to ask are (1) What produces the relativistic plasma? and (2) What energy source powers the kiloparsec-scale outflows?

4.2.1. *Jets from the Active Nucleus*

A small subset of Seyfert galaxies is known to have nuclear jets (see, e.g., Ulvestad, Neff, & Wilson 1987 [NGC 1068], Harrison et al. 1986 [NGC 4151], and Kukula et al. 1993 [Mrk 3]). One would like to know if such jets are ubiquitous in Seyferts and if they are associated with the large-scale radio structures.

If the large-scale radio structures are from jets, how does one explain the fact that large-scale radio structures in Seyferts are not, in general, aligned with nuclear "linear" radio structures (see, e.g., Baum et al. 1993)? One possibility is that subkiloparsec jets are diverted by dense gas clouds in the nuclear region. Such a scenario has been proposed for the bending of the radio jet in NGC 1068 (Gallimore, Baum, & O'Dea 1996). If the jet manages to plow through the dense nuclear environment and continues to flow outward, it might then be affected by ram pressure from rotating gas in the galaxy disk. This effect may be responsible for the Z-shaped optical and radio structures in NGC 3516 (Miyaji, Wilson, & Pérez-Fournon 1992; Mulchaey et al. 1992). Jets that are deflected by gas clouds or ram pressure from the galaxy disk will not emerge from the nuclear region at $\Delta \approx 0°$. This is consistent with our result that, for our sample Seyferts, $\Delta \gtrsim 40°$ (§ 4.1.5). If jets in Seyferts are, in general, weaker than those in radio galaxies, they may lose enough momentum so that they never make their way out of the nuclear region. This may explain the relatively high "core-to-lobe" ratios we found for our Seyfert galaxies (§ 4.1.2).

On the other hand, if the outflows do have sufficient momentum to blow out to larger radii (perhaps as a wind), buoyancy forces may align the outflows so that they continue flowing out roughly perpendicular to the galaxy disk.

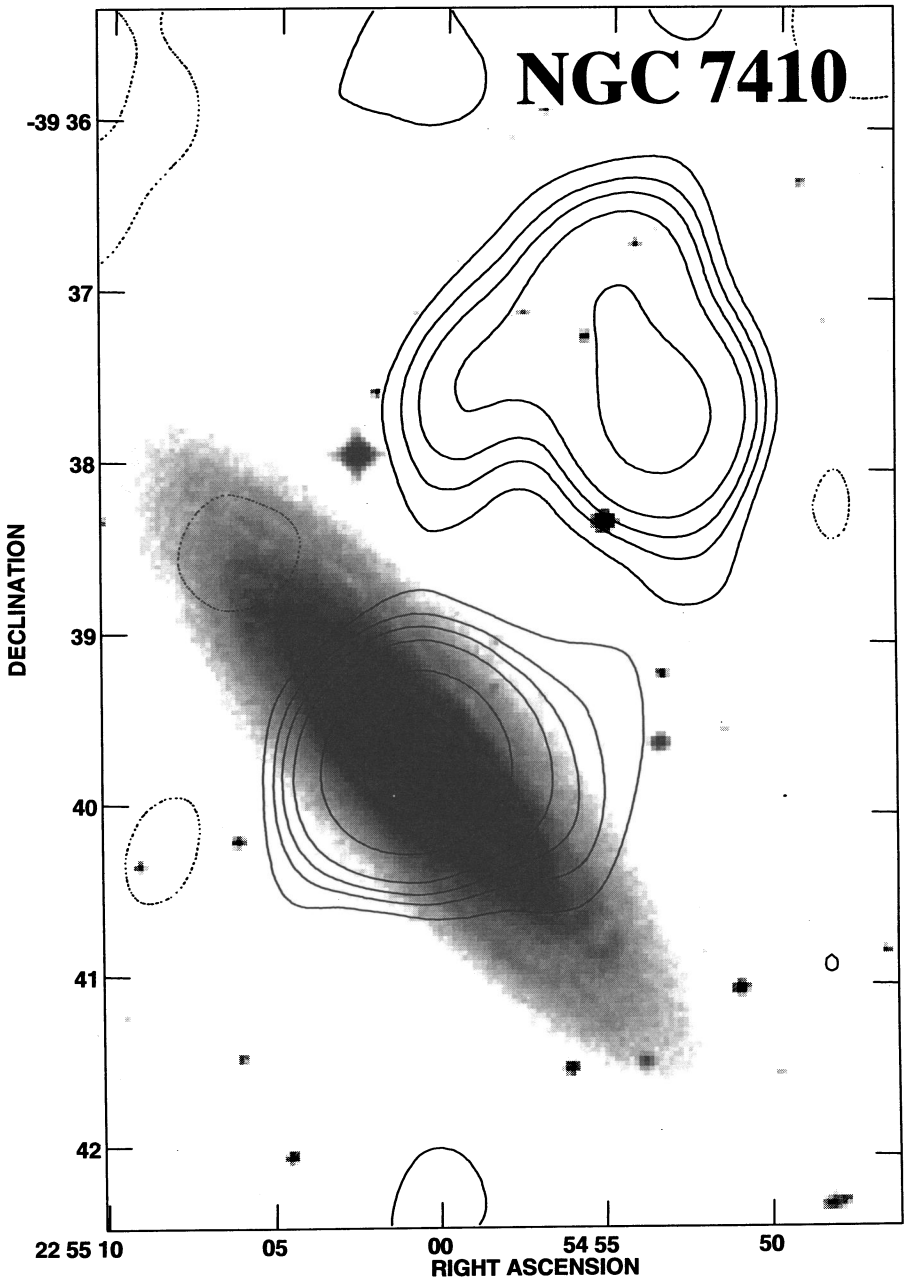

FIG. 1*n*

This may explain why the large-scale radio sources in the Seyferts of Baum et al. (which had larger total radio powers than ours) were apparently preferentially oriented along the galaxy minor axes. A specific example of where buoyancy forces may have redirected the outflow can be found in NGC 4388. The (subkiloparsec) linear nuclear radio source is oriented at P.A. $\approx 25°$. Saikia & Hummel (1989) show that diffuse emission extends from this linear source in the direction of the minor axis (P.A. 0°). This diffuse emission is most likely connected with the large-scale radio structures, which are oriented along the same P.A. (see Fig. 1*h*; Stone et al. 1988).

Another possibility is that the AGN drives a wide-angled wind. If the jet flow is stopped in the nuclear region, the energy from the jet will rapidly thermalize, and a wind with properties very similar to those of a starburst-driven "superwind" could be driven outward.

4.2.2. *Outflow from a Nuclear Starburst*

There seems to be good evidence that nuclear star formation is fairly common in Seyferts (NGC 1068: Balick & Heckman 1985; NGC 4388: Corbin et al. 1988, Stone et al. 1988; NGC 4945: Heckman et al. 1990; NGC 7469: Wilson et al. 1986, 1991; Mrk 231: Hamilton & Keel 1987, Lipari, Colina, & Macchetto 1994; Rodríguez-Espinosa et al. 1987). Therefore, to some degree, relativistic plasma will be present in the nuclear region, in the SNRs themselves, and in the surrounding interstellar medium. If a strong nuclear starburst is present, it could drive a wide-angled wind out along the galaxy rotation axis, away from the nuclear region. Such a wind will carry some of the plasma (including any produced by the active nucleus) out to kiloparsec scales above the disk. If the nuclear star formation is not strong enough to power a wind, star formation could still be an

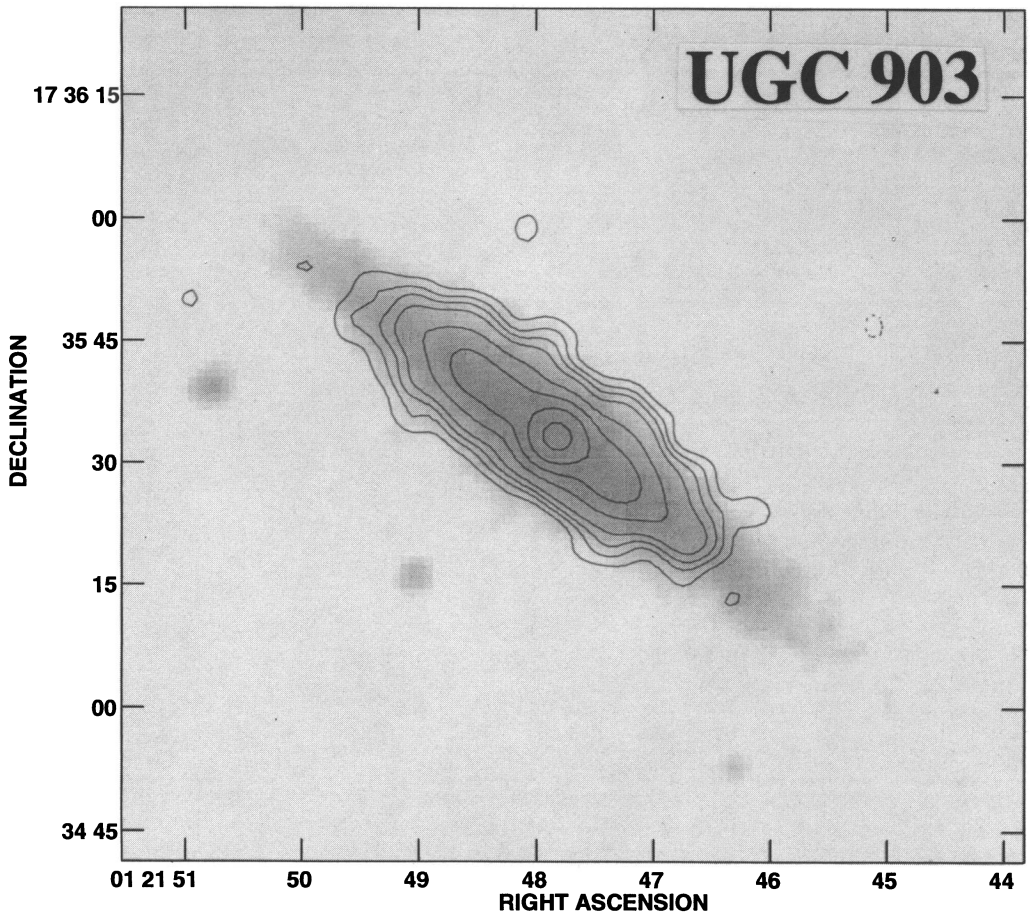

FIG. 2a

FIG. 2.—Large-scale radio maps of edge-on starburst galaxies: As in Fig. 1, contour maps are overlaid on gray-scale plots of the optical emission (images from the STScI digitized sky survey). See § 2 for a description of the "normal" and "tapered" 6 cm maps. Unless otherwise stated, contour levels are 25 μJy × -3, 3, 5, 7, and 10 and then successive levels are a factor of 2 larger. (*a*) UGC 903. Normal map. The peak flux density is 5.0 mJy beam^{-1}. (*b*) NGC 1134. Normal map. The peak flux density is 5.4 mJy beam^{-1}. (*c*) NGC 3044. Normal map. On facing page, tapered (*upper*) map plus reproduction of the 20 cm map (18″ beam) from Condon et al. (1990) (*lower*). Peak flux densities in the normal and tapered maps are 3.2 and 6.6 mJy beam^{-1}, respectively. The lowest contour levels in the 20 cm map is 0.5 mJy beam^{-1}, and successive levels are a factor of $2^{1/2}$ larger in flux density. (*d*) NGC 7541. Normal map. The peak flux density is 12.1 mJy beam^{-1}.

important influence on the large-scale radio sources, as the relativistic plasma produced by the starburst could be carried out to kiloparsec scales by an AGN-driven jet.

Assuming the supernova rate scales with nonthermal radio power, we can estimate upper limits for the supernova rates for putative starbursts in Seyferts. Radio powers of $P_6 \sim 10^{20.3}$–$10^{22.3}$ W Hz^{-1} (Table 1) corresponds with supernova rates of $\sim 10^{-2.3}$ to $10^{-0.3}$ yr^{-1} (see Condon & Yin 1990). Most of the radio emission in Seyferts originates from the nuclear region and, in some cases, D-type sources, which are probably associated with star formation (Wilson 1988), dominate the nuclear radio luminosities. Thus, it is feasible that starburst-driven winds may be present in some Seyferts. As an example, a starburst with a supernova rate of $10^{-2.3}$ yr^{-1} will drive a galactic wind with kinetic luminosity $\sim 10^{41.2}$ ergs s^{-1} (see Heckman et al. 1990), which is consistent with our estimates of kinetic luminosities of LSOs from Paper I.

As mentioned previously, in general, the large-scale radio sources in the Seyferts in our sample do not have spherical halo-like morphologies, as in starburst galaxies. Furthermore, the radio sources are not strongly oriented along the galaxy minor axes (i.e., $\Delta \sim 40°$–$90°$). Hence, if the outflows are starburst-driven winds, either they are collimated somehow as they emerge from the nuclear region or it is only that the radio structures appear to be from collimated outflows. An important distinction to make between winds in starburst galaxies and those envisaged for Seyferts is that the winds in Seyferts would originate from a much smaller region around the nucleus ($\lesssim 1$ kpc, compared to several kiloparsecs in starburst galaxies). Thus, at small radii, the radio morphology of a starburst-driven wind in a Seyfert may resemble that from a collimated outflow. On slightly larger scales, circumnuclear tori of dense gas clouds, which are known to be present in some Seyferts (e.g., the kiloparsec-scale molecular ring in NGC 1068), may collimate a starburst-driven wind by blocking gas that flows out along the disk. If the circumnuclear gas clouds are not uniformly distributed in a torus, the outflow could emerge from the nuclear region at a skewed angle with respect to the galaxy disk. For example, if a wind encounters individual gas clouds that are positioned so as to directly block the outflow perpendicular to the galaxy disk, the radio structure of the wind might resemble what we observe in the Seyferts: diffuse morphologies that are not preferentially oriented along the galaxy minor axes.

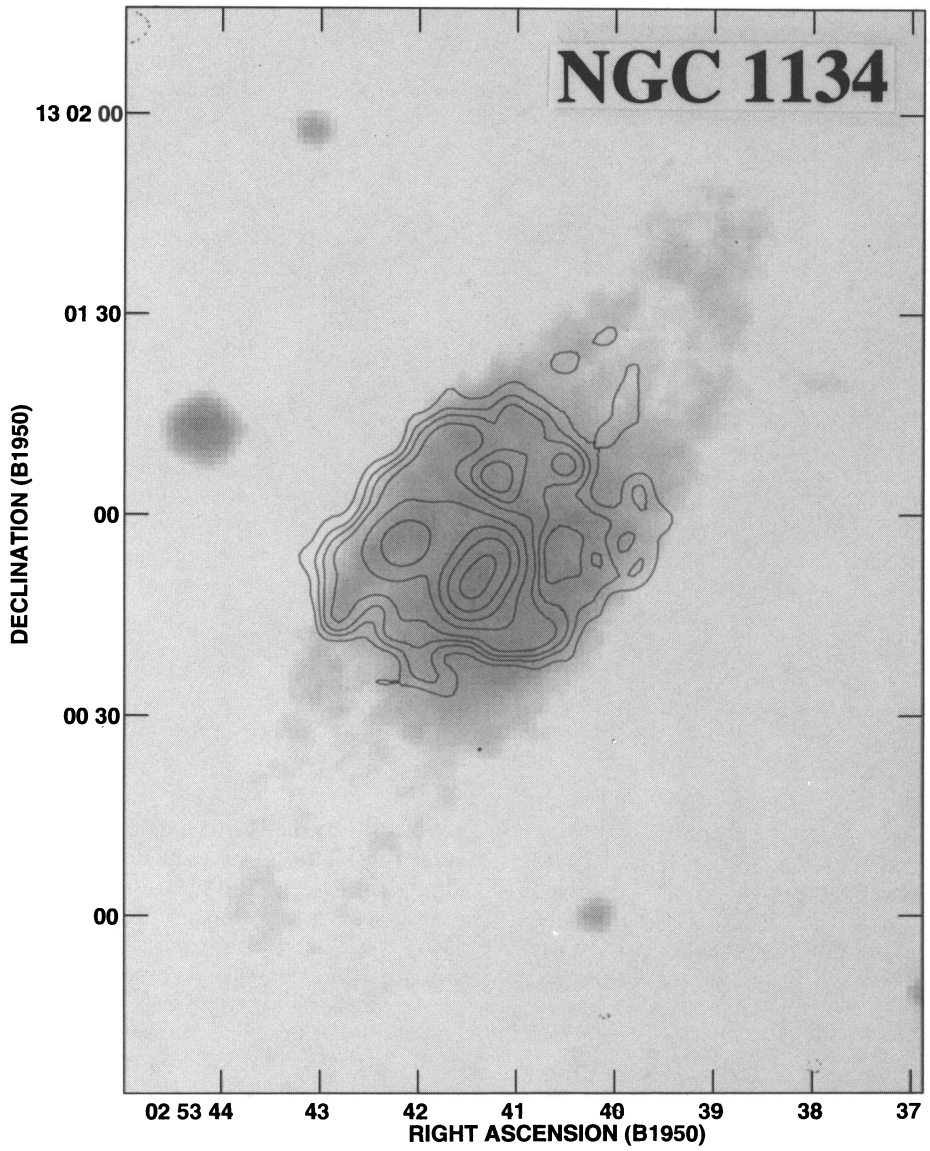

FIG. 2*b*

It is also possible that the observed radio emission does not accurately trace the outflow but represents only regions of high column density of synchrotron-emitting electrons, such as an edge of an expanding bubble.

However, it is difficult to explain how a starburst-driven wind could produce large-scale radio sources that are bisymmetric with respect to the nucleus but are not oriented perpendicular to the major axis. Only the scenario in which the active nucleus is itself a powerful starburst (see, e.g., Terlevich 1992) and the "wind" is collimated by a thick gas torus (such as is proposed in unified models for AGN; see Antonucci 1993) would seem to apply. Such bisymmetric radio morphologies, like that in NGC 4235, are more suggestive of the presence of a collimated outflow from the active nucleus.

If star formation activity produces a significant fraction of the radio power in Seyferts, one might expect the radio and far-IR luminosities to be correlated as in starburst galaxies (see, e.g., Helou et al. 1985). For the Seyferts in our complete sample (Table 1), μ, the logarithm of the ratio of 6 cm radio flux to 60 μm flux, has mean value and dispersion 2.3 ± 0.4. For our four starburst galaxies, the correlation is much tighter (2.50 ± 0.06), consistent with results for a much larger sample of IR-bright galaxies from Condon & Broderick (1988; 2.45 ± 0.3). As expected, $\langle\mu\rangle$ is smaller for the Seyferts since the AGN produces some of the radio emission.

By subtracting the power of the linear nuclear radio sources from the total radio power, Baum et al. (1993) calculated "extranuclear" radio powers and computed corrected values of μ ("μ_{XN}"). They found that mean value of μ then shifted upward so that it was consistent with the mean value of μ for starbursts (although the Seyferts had larger dispersion in μ by a factor ≈ 3). If we attempt a similar correction (substituting P_{XN} [Table 4] for P_T), we find that the distribution of μ_{XN} also shifts upward (2.6 ± 0.6; however, one must be cautioned that, in our calculation we have also subtracted any nuclear diffuse [D-type] emission that may have been present in the nuclear region). Since the two distributions of μ and μ_{XN} for our sample overlap considerably (and both include the starburst value $\mu = 2.5$), we cannot suggest (or deny) that P_{XN} is produced by star formation

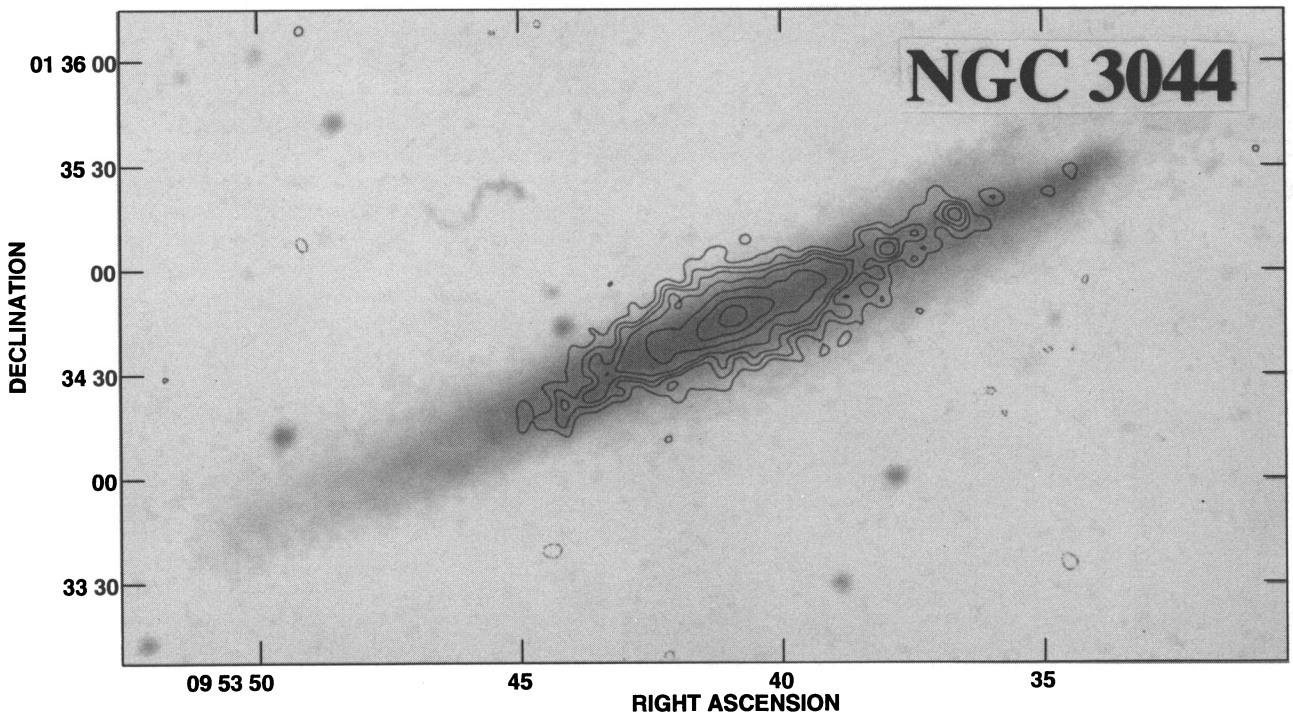

FIG. 2c

activity. A more conclusive test could be done by subtracting only radio powers corresponding to nuclear radio sources produced by the active nucleus (e.g., unresolved cores and subkiloparsec linear structures). Unfortunately, high-resolution radio maps are not available for most of the Seyferts in our sample.

5. SUMMARY AND CONCLUSIONS

As part of our program to study large-scale outflows (LSOs) in Seyfert galaxies, we have obtained deep radio continuum images at 4.9 GHz (6 cm) with the VLA of 10 galaxies from our complete sample of edge-on Seyfert galaxies (Paper I) and four edge-on starburst galaxies that are well matched to the Seyferts in radio luminosity, axial ratio, and recessional velocity. These radio maps and previously published maps from the literature are used to investigate the nature and origin of kiloparsec-scale radio structures in Seyferts.

We found that six of the 10 Seyferts observed have large-scale radio structures extending $\gtrsim 1$ kpc from the nucleus. All four starburst galaxies have a very bright disk component, and one has evidence for a radio halo that extends out of the galaxy plane. In the Seyfert galaxies, most of the radio emission is, in general, concentrated in the nuclear region ($\lesssim 1$ kpc). In our starburst galaxies (which have comparable total radio luminosity), the surface brightness of the outer disk is much brighter than that in the Seyferts.

We found luminous (6 cm radio powers ~ 1–8×10^{19} W Hz^{-1}), unresolved radio sources in the disks of five of the 10 Seyfert galaxies. Follow-up studies are warranted to determine if these sources are radio supernovae or groups of supernova remnants.

Large-scale radio sources in Seyferts typically extend out to radii ~ 1–5 kpc and have radio powers and radial extents similar to those of radio halos in starburst galaxies. In general, the large-scale radio sources are not oriented perpendicular to the major axis but appear to emerge from the galaxy disk at a skewed angle. Their morphologies resemble diffuse emission from a collimated outflow originating in the nuclear region and not a spherical halo extending out along the galaxy minor axis. The large-scale radio sources are often (but not always) associated with optical emission-line regions and kinematically disturbed gas.

Although the active nucleus could easily both produce the relativistic plasma and provide sufficient energy for driving the outflow, nuclear starbursts are also capable of doing so. Our result that large-scale radio structures are not preferentially oriented perpendicular to the galaxy major axes suggests that LSOs are not spherical winds blowing out of the nuclear region. The observed large-scale radio structures are most easily understood in the context of a directed outflow (e.g., an AGN-driven jet) that is somehow diverted away from the galaxy disk on scales $\gtrsim 1$ kpc. Future observational studies of LSOs in individual Seyfert galaxies are needed in order to distinguish among all of the scenarios that may be occurring in the nuclear region. Such studies may also shed light on the relationship (if any exists) between classical starburst galaxies, powerful radio galaxies, and Seyfert galaxies.

E. J. M. C. would like to thank Michael Dahlem, Alan Roy, and Brian Rush for providing helpful information and for useful discussions. E. J. M. C. acknowledges support from the Director's Office of the Space Telescope Science Institute and NASA grant NAG5-3016. This research has made extensive use of the NASA/IPAC Extragalactic Database (NED), which is operated by the Jet Propulsion Laboratory, Caltech, under contract with NASA. This paper represents a portion of E. J. M. C.'s Ph.D. thesis, to be submitted in partial fulfillment of the requirements of the Graduate School of the University of Maryland.

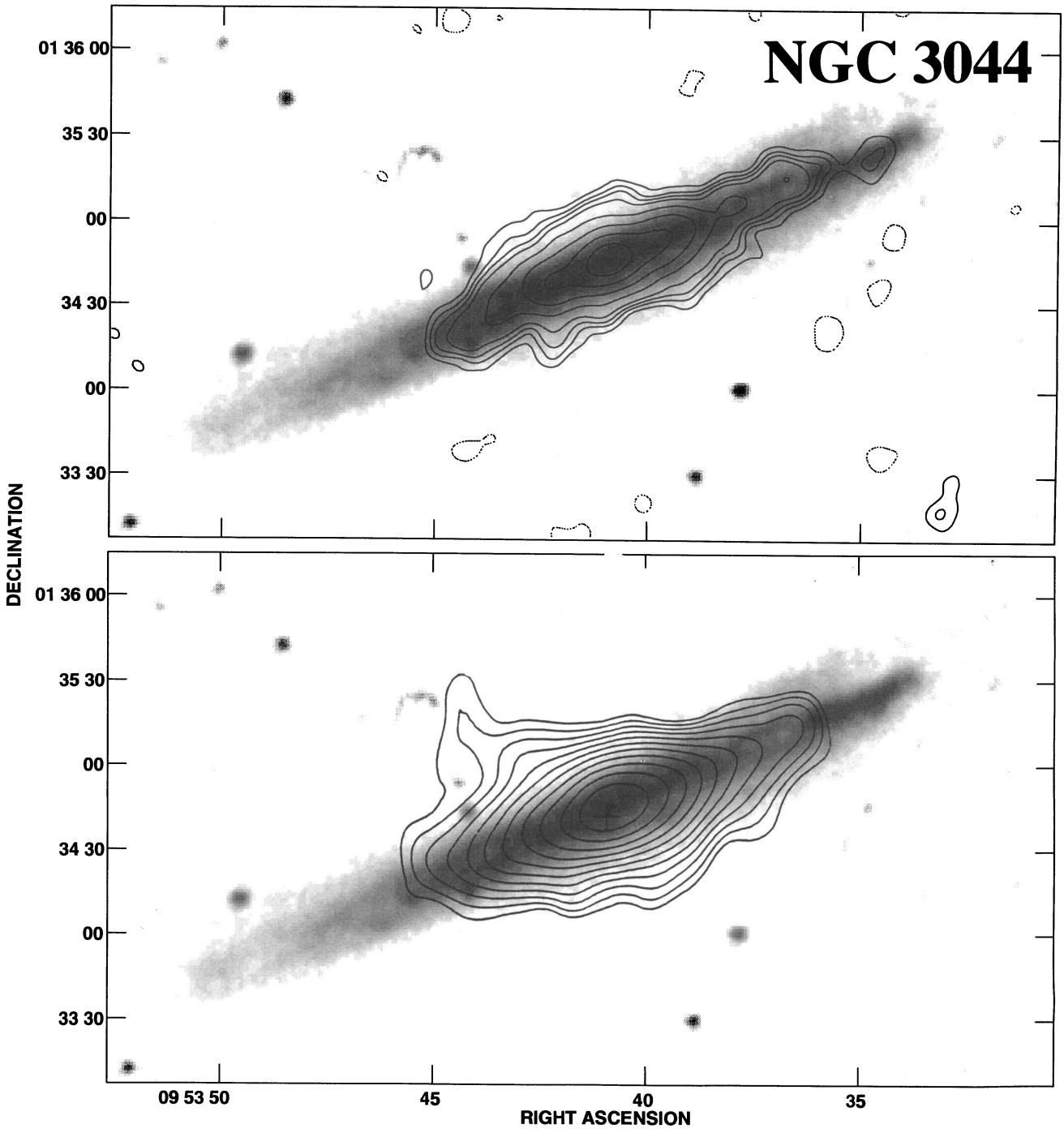

FIG. 2c—*Continued*

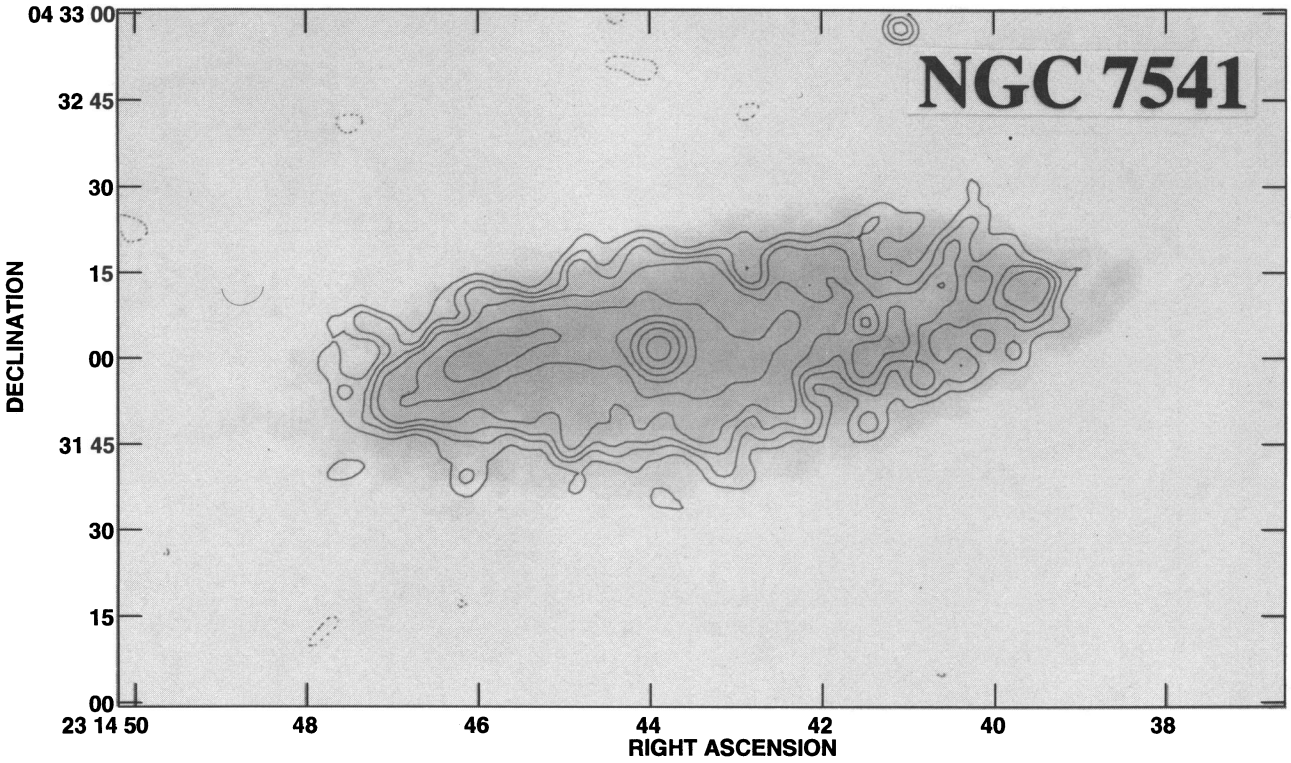

FIG. 2*d*

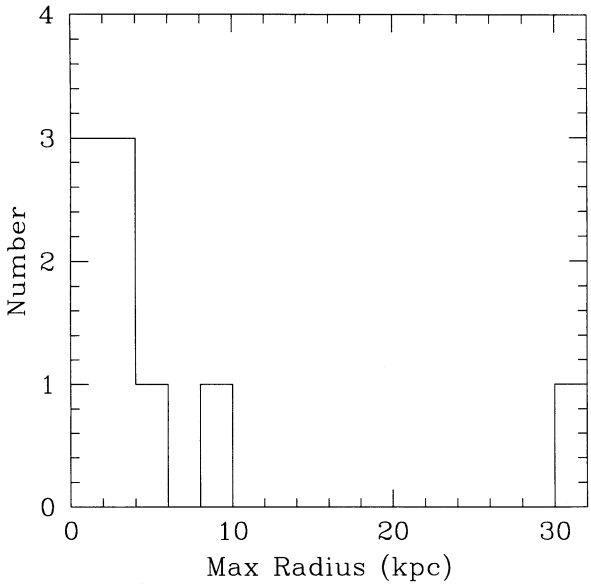

FIG. 3.—Histogram of the maximum projected radius of large-scale radio structures in Seyferts. Values were taken for the nine Seyferts listed in Table 5.

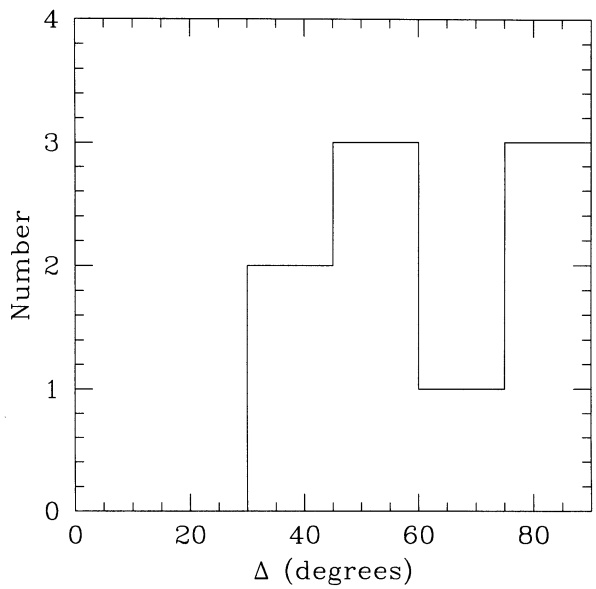

FIG. 4.—Orientation of the large-scale radio structures in Seyferts. Histogram of Δ, the angle between the large-scale emission and the galaxy major axis. Values were taken for the nine Seyferts listed in Table 5.

APPENDIX A

THE SEYFERT GALAXY IRAS 13197−1627 IS MCG −3-34-64

In Figure 5, we show contour maps of the 4.9 GHz radio emission from the two galaxies MCG −3-34-63 and MCG −3-34-64. We find total radio fluxes of 93.4 mJy (5.0×10^{22} W Hz^{-1} at an assumed distance of 67.2 Mpc) and 1.3 mJy (7.1×10^{20} W Hz^{-1}) for MCG −3-34-63 and MCG −3-34-64, respectively. The central source in MCG −3-34-63 has a flux of 0.6 mJy (3.4×10^{20} W Hz^{-1}), and the source positioned ~15″ (4.9 kpc) northeast of the nucleus has a flux of 0.15 mJy (8.1×10^{19} W Hz^{-1}). The radio source in MCG −3-34-64 is slightly resolved along P.A. 135°.

Our complete sample of edge-on Seyfert galaxies was constructed by cross-referencing various Seyfert catalogs with RC3 (de Vaucouleurs et al. 1991; see Paper I). One of the objects selected by this process was the warm FIR galaxy IRAS 13197−1627, which is listed in the Seyfert catalog of Huchra (1995). This object was first identified as a Seyfert galaxy by de Grijp et al. (1985). Several workers have associated this *IRAS* source with MCG −3-34-63, an edge-on galaxy with axial ratio 3.2 (RC3). We have since found that IRAS 13197−1627 is not associated with MCG −3-34-63 but is instead associated with the galaxy MCG −3-34-64, positioned ~1.′8 southeast of MCG −3-34-63.

We suspected this to be the case when we found a large disagreement between our observed radio fluxes for MCG −3-34-63 and those listed in the literature from previous radio observations (which were undoubtedly measurements of the stronger radio source MCG −3-34-64). The *IRAS* fluxes listed for IRAS 13197−1627 (which probably include emission from both galaxies) also implied excessively large values of μ (i.e., the FIR flux was comparatively very large). We later learned (M. de Robertis 1995, private communication) that the nuclear spectrum which identified the Seyfert galaxy IRAS 13197−1627 is a spectrum of MCG −3-34-64, not MCG −3-34-63.

Authors of future catalogs of Seyferts should note that this error has progressed into many published catalogs and papers.

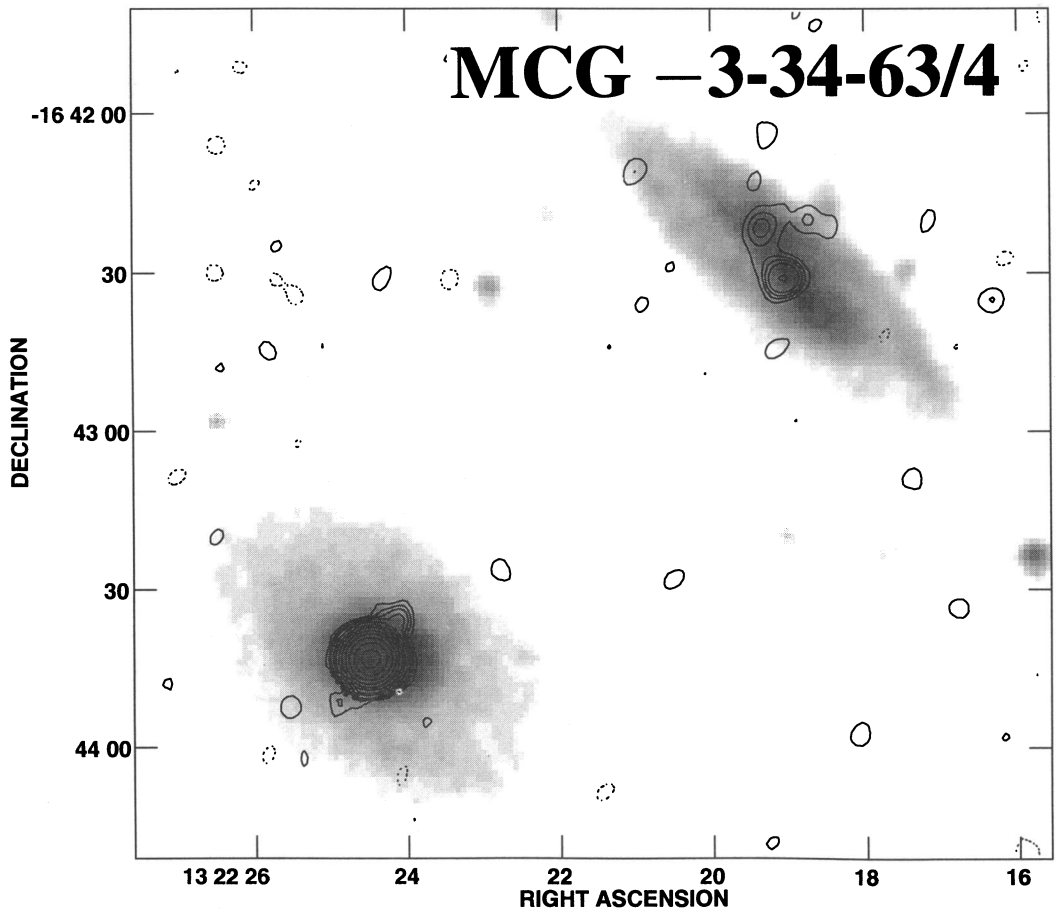

FIG. 5.—Normal (see § 2) radio map overlaid on a gray-scale plot of an optical image from the STScI digitized sky survey. The edge-on galaxy MCG −3-34-63 is located in the upper right of the image, whereas the Seyfert galaxy MCG −3-34-64 is located in the lower left. Contour levels are 25 μJy × −3, 3, 5, 7, and 10 and then successive levels are a factor of 2 larger. The peak flux density is 89.9 mJy beam^{-1}.

REFERENCES

Antonucci, R. R. J. 1993, ARA&A, 31, 473
Balick, B., & Heckman, T. M. 1985, AJ, 90, 197
Baum, S. A., O'Dea, C. P., Dallacassa, D., de Bruyn, A. G., & Pedlar, A. 1993, ApJ, 419, 553
Carilli, C. L., Holdaway, M. A., Ho, P. T. P., & de Pree, C. G. 1992, ApJ, L59
Colbert, E. J. M., Baum, S. A., Gallimore, J. F., O'Dea, C. P., Lehnert, M. D., Tsvetanov, Z. I., Mulchaey, J. S., & Caganoff, S. 1996, ApJS, 105, 75 (Paper I)
Condon, J. J. 1987, ApJS, 65, 485
———. 1992, ARA&A, 30, 575
Condon, J. J., & Broderick, J. J. 1988, AJ, 96, 30
Condon, J. J., Condon, M. A., Gisler, G., & Puschell, J. J. 1982, ApJ, 242, 102
Condon, J. J., Helou, G., Sanders, D. B., & Soifer, B. T. 1990, ApJS, 73, 359
Condon, J. J., & Yin, Q. F. 1990, ApJ, 357, 97
Corbin, M. R., Baldwin, J. A., & Wilson, A. S. 1988, ApJ, 334, 584
Dahlem, M., Lisenfeld, U., & Golla, G. 1995, ApJ, 444, 119
de Bruyn, A. G., & Wilson, A. S. 1976, A&A, 53, 93
de Grijp, Miley, G. K., Lub, J., & de Jong, T. 1985, Nature, 314, 240
de Vaucouleurs, G., de Vaucouleurs, A., Corwin, H. G., Buta, R. J., Paturel, G., & Fouque, P. 1991, Third Reference Catalog of Bright Galaxies (New York: Springer) (RC3)
Edelson, R. A. 1987, ApJ, 313, 651
Fullmer, L., & Lonsdale, C. 1989, Cataloged Galaxies and Quasars in the *IRAS* Survey (JPL Pub. D-1932, Version 2, Appendix B)
Gallimore, J. F., Baum, S. A., & O'Dea, C. P. 1996, ApJ, 464, 198
Hamilton, D., & Keel, W. C. 1987, ApJ, 321, 211
Harnett, J. I., Haynes, R. F., Klein, U., & Wielebinski, R. 1989, A&A, 216, 39
Harrison, B., Pedlar, A., Unger, S. W., Burgess, P., Graham, D. A., & Preuss, E. 1986, MNRAS, 218, 775
Heckman, T. M., Armus, L., & Miley, G. K. 1990, ApJS, 74, 833
Helou, G., Soifer, B. T., & Rowan-Robinson, M. 1985, ApJ, 298, L7
Huchra, J. 1995, private communication (updated electronic version of Catalogue of Seyfert Galaxies and Other Bright AGN)
Hummel, E. 1981, A&A, 93, 93
Hummel, E., Beck, R., & Dettmar, R.-J. 1991, A&AS, 87, 309
Hummel, E., & van der Hulst, J. M. 1989, A&AS, 81, 51
Hummel, E., van Gorkom, J., & Kotanyi, C. 1983, ApJ, 267, L5
Kojoian, G., Tovmassian, H. M., Dickinson, D. F., & St. Clair Dinger, A. 1980, AJ, 85, 1462
Kukula, M. J. 1993, Ph.D. thesis, Univ. of Manchester
Kukula, M. J., Ghosh, T., Pedlar, A., Schilizzi, R. T., Miley, G. K., de Bruyn, A. G., & Saikia, D. J. 1993, MNRAS, 264, 893
Kukula, M. J., Pedlar, A., Baum, S. A., & O'Dea, C. P. 1995, MNRAS, 276, 1262
Lehnert, M. D., & Heckman, T. M. 1995, ApJS, 97, 89
Lipari, S., Colina, L., & Macchetto, F. 1994, ApJ, 427, 174
Meurs, E. J. A., & Wilson, A. S. 1981, A&AS, 45, 99
———. 1984, A&A, 136, 206
Miyaji, T., Wilson, A. S, & Pérez-Fournon, I. 1992, ApJ, 385, 137
Moshir, M., et al. 1992, Explanatory Supplement to the *IRAS* Faint Source Catalog, version 2, JPL D-10015 (Pasadena: JPL)
Mulchaey, J. 1995, private communication
Mulchaey, J. S., Tsvetanov, Z., Wilson, A. S., & Pérez-Fournon, I. 1992, ApJ, 394, 91
Perley, R. A., Schwab, F. R., & Bridle A. H., ed. 1989, ASP Conf. Proc. 6, Synthesis Imaging in Radio Astronomy (San Francisco: ASP)
Pogge, R. W. 1989, ApJ, 345, 730
Rodríguez-Espinosa, J. M., Rudy, R. J., & Jones, B. 1987, ApJ, 312, 555
Rush, B., Malkan, M. A., & Edelson, R. A. 1995, ApJ, submitted
Rush, B., Malkan, M. A., & Spinoglio, L. 1993, ApJS, 89, 1
Saikia, D. J., & Hummel, E. 1989, in Extranuclear Activity in Galaxies, ed. E. Meurs & R. Fosbury (Garching: ESO), 165
Seaquist, E. R., & Odegard, N. 1991, ApJ, 369, 320
Stone, J. L., Jr., Wilson, A. S., & Ward, M. J. 1988, ApJ, 330, 105
Sramek, R. A., & Weiler, K. W. 1990, in Supernovae, ed. A. G. Petschek (New York: Springer), chap. 4
Terlevich, R. 1992, in ASP Conf. Proc. 31, Relationships between Active Galactic Nuclei and Starburst Galaxies, ed. A. Filippenko (San Francisco: ASP), p. 133
Tsvetanov, Z., Dopita, M., & Allen, M. 1995, BAAS, 26(5), 871
Ulvestad, J. S., Neff, S. G., & Wilson, A. S. 1987, AJ, 93, 92
Ulvestad, J. S., & Wilson, A. S. 1984, ApJ, 285, 439
———. 1989, ApJ, 343, 659
Ulvestad, J. S., Wilson, A. S., & Sramek, R. A. 1981, ApJ, 247, 419
Unger, S. W., Lawrence, A., Wilson, A. S., Elvis, M., & Wright, A. E. 1987, MNRAS, 228, 521
Unger, S. W., Pedlar, A., Booler, R. V., & Harrison, B. A. 1986, MNRAS, 219, 387
Unger, S. W., Wolstencroft, R. D., Pedlar, A., Savage, A., Clowes, R. G., Legett, S. K., & Parker, Q. A. 1989, MNRAS, 236, 425
van der Laan, H., & Perola, G. C. 1969, A&A, 3, 468
Ward, M. J., Penston, M. V., Blades, J. C., & Turtle, A. J. 1980, MNRAS, 193, 563
Weaver, K. A., Wilson, A. S., & Baldwin, J. A. 1991, ApJ, 366, 50
Wehrle, A. E., & Morris, M. 1987, ApJ, 313, L43
———. 1988, AJ, 95, 1689
Wilson, A. S. 1988, A&A, 206, 41
Wilson, A. S., Baldwin, J. A., Sun, S.-D., & Wright, A. E. 1986, ApJ, 310, 121
Wilson, A. S., Baldwin, J. A., & Ulvestad, J. S. 1985, ApJ, 291, 627
Wilson, A. S., Elvis, M., Lawrence, A., & Bland-Hawthorn, J. 1992, ApJ, 391, L75
Wilson, A. S., Helfer, T. T., Haniff, C. A., & Ward, M. J. 1991, ApJ, 381, 79
Wilson, A. S., & Meurs, E. J. A. 1982, A&AS, 50, 217
Wilson, A. S., & Penston M. V. 1979, ApJ, 232, 389
Wilson, A. S., & Willis, A. G. 1980, ApJ, 240, 429
Wright, A. E. 1974, MNRAS, 167, 273
Zirbel, E. L., & Baum, S. A. 1995, ApJ, 448, 521